



Discovery of selective fragment-sized immunoproteasome inhibitors

Levente Kollár^{a,1}, Martina Gobec^{b,1}, Bence Szilágyi^a, Matic Proj^b, Damijan Knez^b, Péter Ábrányi-Balogh^a, László Petri^a, Tímea Imre^c, Dávid Bajusz^a, György G. Ferenczy^a, Stanislav Gobec^b, György M. Keserű^{a,**}, Izidor Sosič^{b,*}

^a Medicinal Chemistry Research Group, Research Centre for Natural Sciences, Magyar tudósok krt. 2, H-1117, Budapest, Hungary

^b University of Ljubljana, Faculty of Pharmacy, Aškerčeva cesta 7, SI-1000, Ljubljana, Slovenia

^c MS Metabolomics Research Group, Research Centre for Natural Sciences, Magyar tudósok krt. 2, H-1117, Budapest, Hungary

ARTICLE INFO

Article history:

Received 14 December 2020

Received in revised form

14 March 2021

Accepted 5 April 2021

Available online 20 April 2021

Keywords:

Immunoproteasome

Fragments

Chloro scan

Thiones

Disulfide formation

Electrophilic warheads

ABSTRACT

Proteasomes contribute to maintaining protein homeostasis and their inhibition is beneficial in certain types of cancer and in autoimmune diseases. However, the inhibition of the proteasomes in healthy cells leads to unwanted side-effects and significant effort has been made to identify inhibitors specific for the immunoproteasome, especially to treat diseases which manifest increased levels and activity of this proteasome isoform. Here, we report our efforts to discover fragment-sized inhibitors of the human immunoproteasome. The screening of an in-house library of structurally diverse fragments resulted in the identification of benzo[d]oxazole-2(3H)-thiones, benzo[d]thiazole-2(3H)-thiones, benzo[d]imidazole-2(3H)-thiones, and 1-methylbenzo[d]imidazole-2(3H)-thiones (with a general term benzoXazole-2(3H)-thiones) as inhibitors of the chymotrypsin-like ($\beta 5i$) subunit of the immunoproteasome. A subsequent structure-activity relationship study provided us with an insight regarding growing vectors. Binding to the $\beta 5i$ subunit was shown and selectivity against the $\beta 5$ subunit of the constitutive proteasome was determined. Thorough characterization of these compounds suggested that they inhibit the immunoproteasome by forming a disulfide bond with the Cys48 available specifically in the $\beta 5i$ active site. To obtain fragments with biologically more tractable covalent interactions, we performed a warhead scan, which yielded benzoXazole-2-carbonitriles as promising starting points for the development of selective immunoproteasome inhibitors with non-peptidic scaffolds.

© 2021 Elsevier Masson SAS. All rights reserved.

1. Introduction

In the past two decades, a critical role for the ubiquitin-proteasome system (UPS) has been established in essentially all key cellular processes, including immune response [1,2], cell cycle progression [3,4], regulation of transcription [5,6], genome integrity [7,8], and apoptosis [9]. The central role within the UPS is performed by the 26S proteasome and this includes the rapid degradation of misfolded and damaged proteins and the slower degradation of most other cellular proteins [10]. This makes the proteasome essential for protein homeostasis and of significant physiological importance. Given the immense amount of literature,

the reader is referred to recent reviews [11,12] for further in-depth information on the pharmacology of proteasomes.

The constitutive form of the 26S proteasome consists of a 20S core particle (CP) that has regulatory 19S moieties attached at both ends. The 20S CP is a 720 kDa large barrel-shaped structure assembled of four stacked rings, each consisting of seven subunits [13]. The two outer α -rings are devoid of catalytic activity but provide structural integrity of the protein and form a channel, through which the substrate enters the two inner β -rings [14,15]. The latter are carriers of the proteolytic activity [16,17], because each ring contains three catalytically active subunits that break down proteins. The $\beta 5$ subunit (chymotrypsin-like) is responsible for cleaving bonds after hydrophobic residues, the $\beta 1$ subunit (caspase-like) cleaves peptide bonds after acidic residues, whereas the $\beta 2$ subunit (trypsin-like) cleaves the basic residue bonds [18,19].

Two main types of CPs exist in vertebrates, i.e. the constitutive proteasome (cCP), which is found in all cell types, and the immunoproteasome (iCP), which is expressed mainly in cells of

* Corresponding author.

** Corresponding author.

E-mail addresses: keseru.gyorgy@ttk.hu (G.M. Keserű), izidor.sosic@ffa.uni-lj.si (I. Sosič).

¹ These authors contributed equally to this work.

hematopoietic origin. When exposed to inflammatory factors, such as tumor necrosis factor and interferon- γ , the expression of iCP active subunits β (designated as $\beta 1i$, $\beta 2i$, $\beta 5i$), which replace their constitutive counterparts, is induced in non-hematopoietic cells as well [20–23]. It is known that increased expression and activity of both proteasomes can lead to a number of diseases. These include many types of cancer [24–27] inflammatory and autoimmune diseases [28–30], as well as neurological disorders [31]. The cCP and the iCP therefore represent validated targets for the design of new pharmacologically active compounds [32–38]. Because iCP is induced during the above-mentioned disease processes, selective inhibition of its $\beta 5i$ subunit or simultaneous abrogation of both $\beta 1i$ and $\beta 5i$ activities might have great potential for the treatment of iCP-related abnormalities [39–41]. The majority of currently available inhibitors of iCP, however, have a peptidic backbone (Fig. 1) and these molecules are thus prone to poor metabolic stability and low bioavailability leading to lack of oral exposure. In recent years, there were reports from our labs [42–44] and from others [45–48] on the synthesis and biological evaluation of several types of reversible and irreversible non-peptidic inhibitors of the $\beta 5i$ subunit of human iCP (Fig. 1).

Since our goal is to expand the chemical space of non-peptidic iCP inhibitors, the aim of the current study was to use a fragment-based approach to discover novel chemotypes capable of selectively inhibiting the $\beta 5i$ subunit of human iCP. Given the fact that this strategy has not yet been performed with the iCP and based on the very successful examples of fragment-based design of inhibitors against a wide array of pharmacological targets [57], we were hoping to yield hit compounds amenable for possible development into potent inhibitors. Our efforts resulted in the discovery of low-molecular-weight compounds that selectively inhibit the $\beta 5i$ subunit of iCP in the low micromolar range and as such represent tractable fragments for further hit-to-lead development.

2. Results and discussion

2.1. Initial library screening

An in-house library of more than 900 structurally diverse fragments was screened in the $\beta 5i$ inhibition assay using Suc-LLVY-AMC as a fluorogenic substrate (for details see Experimental section). The data were calculated as the residual activities (RAs) of $\beta 5i$ in the presence of 100 μ M of each compound. Fragments that showed more than 50% inhibition of the iCP (52 hits) were subjected to dose-dependent inhibitory activity measurements. Of these, 18 compounds with different structural characteristics showed satisfying and repeatable IC_{50} values and are reported in Table S1. After visual inspection, availability of derivatives and their synthetic feasibility, absence of highly reactive functionalities and possible toxicophores, we selected seven hits (query compounds shown in orange shading in Tables S1 and S2) for further studies. In the initial 'structure-activity relationship (SAR) by catalogue' step, 61 structurally related compounds were purchased and assayed for $\beta 5i$ inhibition (Table S2). Based on these results, four closely related series of molecules were selected for further investigations (Fig. 2).

We are aware that compounds of this structural type can exist in two tautomeric forms due to the iminothiol-thioamide equilibrium. However, it was previously determined by others [58] and confirmed by us [59] that benzimidazole-2-thiones are present predominantly in the thioamide form in solid state and in deuterated DMSO. In addition, it was shown that the thioamide molar fraction in DMSO obtained by ^{15}N NMR for compounds **1**, **2**, and **3** is 1.00, 0.99, and 0.92, respectively [60]. Our ^{13}C NMR study of a compound from the 'thiazole series' showed no change of the spectrum in DMSO versus in DMSO-containing buffer suggesting that the thioamide isomer prevails also in the aqueous environment (Figure S1). This was further supported by the UV-Vis spectra

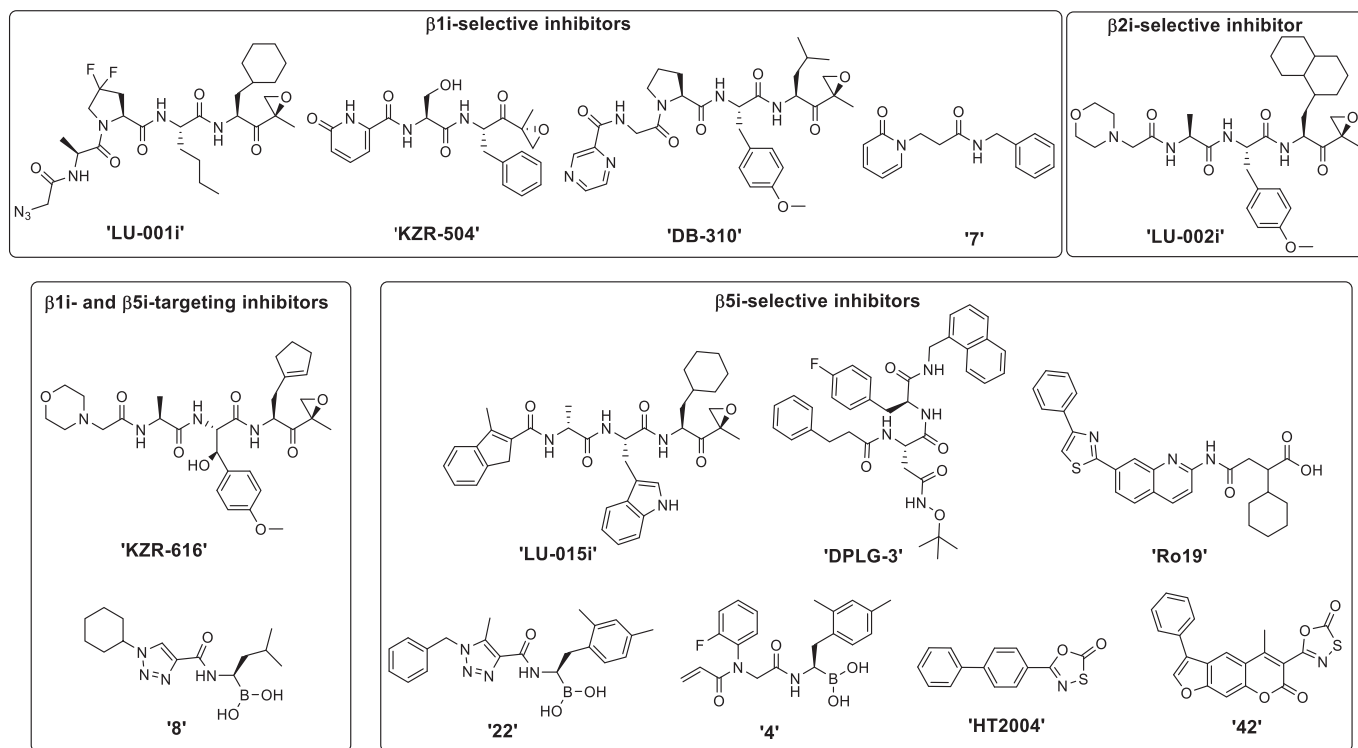


Fig. 1. Representatives of iCP-selective inhibitors disclosed in scientific papers. References to original reports are given here: 'LU-001i' and 'LU-015i' [49], 'KZR-504' [50], 'DB-310' [51], '7' [52], 'LU-002i' [53], 'KZR-616' [54], '4', '8', and '22' [55], 'DPLG-3' [56], 'Ro19' [47], 'HT2004' [45], '42' [42]. For a more thorough overview of the patent literature, the reader is referred to a recent review [39].

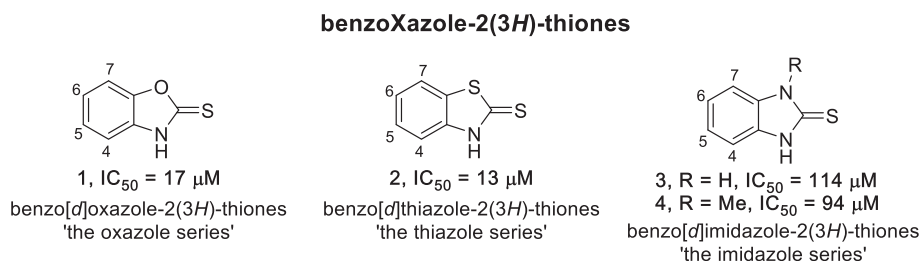


Fig. 2. Parent compounds of the four closely related series after fragment screening and 'SAR by catalogue' investigations. Throughout the manuscript, we use a general term for all four series, i.e. the benzoXazole-2(3H)-thiones. IC₅₀ values are means from at least three independent determinations. Standard deviations were <20% (not shown). Ring numbering is shown to help understanding of the SAR information.

with the appearance of the 320 nm peak, characteristic to the thione group in benzo[d]thiazole-2(3H)-thiones (Figure S2) [61]. For these reasons, we refer to all compounds in this manuscript in the thioamide tautomeric form.

The four series exhibited differences both in the activities of the corresponding parent compounds **1–4** and in their preliminary SAR as shown by data obtained by the 'SAR by catalogue' study (Table S2). For example, the benzo[d]oxazole-2(3H)-thione (**1**) lost activity if thione was changed to oxo (**FRBD5**), if it was replaced with a methylthio substituent (**FRBD8**), and also when thione was replaced with imine (**FRBD13**) or was omitted (**FRBD12**). The benzo[d]thiazole-2(3H)-thione (**2**) also lost activity when thione was replaced with either imine (**FRBD35**) or oxo group (**FRBD38**). In contrast, it was active without the thione (**Query 44/D2**, IC₅₀ = 38 ± 7.9 μM, Table S2). Interestingly, the benzo[d]imidazole-2(3H)-thione (**3**) tolerated the thione to methylthio replacement (**FRBD14**, RA = 21% at 100 μM, IC₅₀ = 92 ± 18 μM) but not the thione to oxo change (**FRBD18**, RA = 109% at 100 μM).

2.2. Chloro scan of thiones

To explore the SAR of benzoXazole-2(3H)-thiones (Fig. 2) in a more systematic way and to gain insights into possible fragment growing vectors, we performed a chloro scan on all accessible positions at the benzene ring of the four parent benzoXazole-2(3H)-thiones **1–4**. The majority of these derivatives (**5–13**) were commercially available, whereas compounds **14–18** were synthesized as described previously [59]. The assay results are shown in Table 1.

The addition of a chlorine atom at positions 4, 5, and 6 of the benzo[d]oxazole-2(3H)-thione scaffold (compounds **5–7**) and at positions 4 and 5 of the benzo[d]thiazole-2(3H)-thione (compounds **9** and **10**) ring led to a small decrease in inhibitory potencies. On the other hand, the substitution at position 7 had a minor influence on the IC₅₀ values in both series since compounds **8** (IC₅₀ = 16 ± 0.4 μM, Table 1) and **12** (IC₅₀ = 9.7 ± 1.9 μM, Table 1) showed similar inhibition in comparison to the parent compounds **1** and **2** (Fig. 2). In the 'imidazole series', the 6- and 7-chloro substitutions resulted in improvements in inhibition (comparison of the parent compound **3** with **13** and **14**, Fig. 2, Table 1), especially for compounds where one of the nitrogen atoms of the benzo[d]imidazole-2(3H)-thione was methylated. Namely, compounds **17** (IC₅₀ = 4.2 ± 0.9 μM, Table 1) and **18** (IC₅₀ = 1.8 ± 0.3 μM, Table 1) showed 20- to 50-fold improvement in inhibition, respectively, in comparison to the parent compound **4** (Fig. 2).

2.3. Expansion of the library of analogs

After the chloro scan, we decided to expand the library of analogs within all four series by further examination of derivatives in

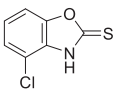
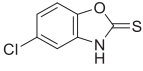
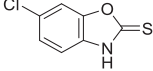
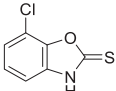
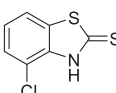
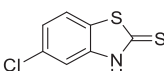
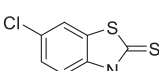
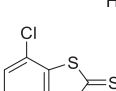
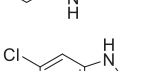
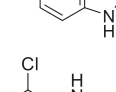
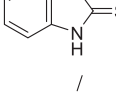
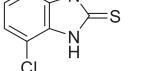
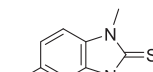
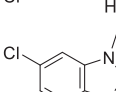
commercially available chemical space, as well as by own synthetic efforts (Schemes 1–3). Based on the assay results of the chloro scan, we focused mainly on derivatives with substituents at positions 6 and 7 of the benzoXazole-2(3H)-thione scaffold. The assay data is summarized in Table 2. For details regarding the characterization of commercially available compounds (**19–37** and **39–41**), please see the Supporting Information. For the preparation of 6-amino-1-methyl-1,3-dihydro-2H-benzo[d]imidazole-2-thione (**42**), 4-nitrobenzene-1,2-diamine (**I**) was used as a starting material (Scheme 1). After monomethylation to obtain **II**, ring closure was performed with 1,1'-thiocarbonyldiimidazole (TCDI), and the resulting 6-nitro compound **38** was hydrogenated using Pd/C as a catalyst. TCDI-mediated cyclization was also used to transform 6-bromo-*N*-1-methylbenzene-1,2-diamine (**III**) into 7-bromo-1-methyl-1,3-dihydro-2H-benzo[d]imidazole-2-thione (**60**), as well as to synthesize 7-nitrobenzo[d]oxazole-2(3H)-thione (**V**) from 2-amino-6-nitrophenol (**IV**). Compound **V** was then reduced using tin(II) chloride to give the desired 7-aminobenzo[d]oxazole-2(3H)-thione (**63**). To obtain 7-amino-1-methyl-1,3-dihydro-2H-benzo[d]imidazole-2-thione (**64**), commercially available *N*-methyl-2,6-dinitroaniline (**VI**) was first catalytically reduced, and the obtained triamine **VII** was reacted with TCDI to give the desired amine **64** (Scheme 1).

For the expansion of the benzoXazole-2(3H)-thione core we selected two types of robust chemistries that include amide coupling and Suzuki reaction [62]. The 6- and 7-amide-substituted benzoXazole-2(3H)-thiones **43–58** and **65–70** were prepared by three different general methods (Scheme 2). If available, we used the anhydrides of desired carboxylic acids as acylation agents and DMAP as a catalyst. In most cases, however, we used the appropriate carboxylic acids and HATU as a coupling agent to prepare desired amide derivatives. Of note, some reactions were performed at elevated temperature (50 °C).

In addition, we synthesized two biaryl-type benzothiazole-2(3H)-thiones **61** and **62** (Scheme 3) by a straightforward three-step synthesis. The reduction of commercially available 2-fluoro-3-bromonitrobenzene (**VIII**) provided the amine **IX**, which was reacted with potassium ethyl xanthate to give the 7-bromobenzo[d]thiazole-2(3H)-thione (**59**). This compound was then used in Suzuki reactions to give 7-aryl-substituted compounds **61** and **62**.

A limited number of derivatives with substitutions at positions 4 and 5 of the benzoXazole-2(3H)-thione scaffolds (compounds **19–28**) precluded proper SAR analyses. Marginal improvement of inhibition in comparison to the parent compound **1** (Fig. 2) was observed for 4-hydroxybenzo[d]oxazole-2(3H)-thione (**22**) with IC₅₀ value of 4.1 ± 0.9 μM (Table 2). Interestingly, the 4-methoxy substitution led to decrease of inhibition of the β5i activity (compound **21**, IC₅₀ = 81 ± 5.0 μM). Methoxy substitution at position 5 in the 'oxazole' and 'thiazole' series was tolerated only in the latter (compound **26**, IC₅₀ = 7.2 ± 6.1 μM), whereas the 5-nitro moiety

Table 1
Inhibitory potencies of compounds obtained with chloro scan against the $\beta 5i$ subunit of human iCP.

Compound	Structure	IC ₅₀ (μ M) ^a
5		36 \pm 4.9
6		96 \pm 9.9
7		65 \pm 3.0
8		16 \pm 0.4
9		43 \pm 12
10		32 \pm 16 ^b
11		nd ^c
12		9.7 \pm 1.9
13		62 \pm 7.8
14		60 \pm 11
15		RA = 50% ^d
16		RA = 80% ^d
17		4.2 \pm 0.9
18		1.8 \pm 0.3

^a IC₅₀ values are means from at least three independent determinations.

^b Approximate value due to low solubility in the assay buffer.

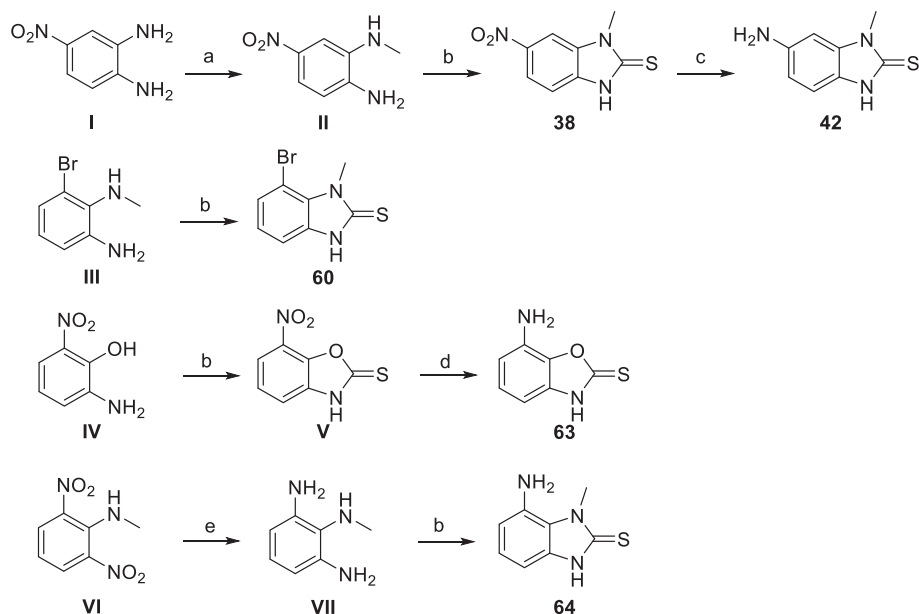
^c Not determined due to very low solubility in DMSO.

^d RA determined at 150 μ M of compound. Standard deviations for RAs were <20%.

resulted in $\beta 5i$ inhibition only in the benzo[d]oxazole-2(3H)-thione scaffold (compound **27**, IC₅₀ = 9.0 \pm 5.0 μ M). For 'oxazole' derivatives with substitution at position 6, only COOMe (**36**, IC₅₀ = 3.0 \pm 1.3 μ M) led to better inhibition in comparison to the parent compound **1** (Fig. 2). Amino group at this position retained inhibitory activity of the compound as observed by the assay result for **39** with IC₅₀ value of 21 \pm 27 μ M. Interestingly, increasing the molecular size of this subclass at position 6 through generation of amide derivatives (compounds **43**, **47**, **50**, **53**, and **56**) abrogated inhibition of the $\beta 5i$ activity (Table 2). All attempts to diversify position 7 within the 'oxazole' series (compounds **63**, **65**, **67**, and **69**) also led to diminished $\beta 5i$ inhibition in comparison to 7-nonsubstituted parent compound **1** (Fig. 2) and 7-chlorobenzo[d]oxazole-2(3H)-thione (**8**, Table 1). Substitution at position 6 within the 'thiazole' derivatives was only marginally beneficial with benzamido moiety (**48**, IC₅₀ = 7.1 \pm 6.0 μ M, Table 2), whereas all other 6-substituted compounds led to either retained (**32**, **34**, **51**), diminished (**30**, **37**, **44**, **54**, **57**), or loss (**40**) of $\beta 5i$ inhibition in comparison to the parent compound **2** (Fig. 2). The activity within 7-substituted 'thiazole' series was retained when Br was attached at that position (compound **59**, IC₅₀ = 11 \pm 1.3 μ M), whereas compounds with aromatic rings at position 7 (**61**, **62**) were either poor $\beta 5i$ inhibitors (**62**) or were poorly soluble (**61**) precluding their IC₅₀ determinations. Surprisingly and in contrast with the results of the chloro scan, all 6- and 7-substituted compounds within both 'imidazole' series resulted in a complete abrogation of inhibitory activity (Table 2, columns 4 and 5).

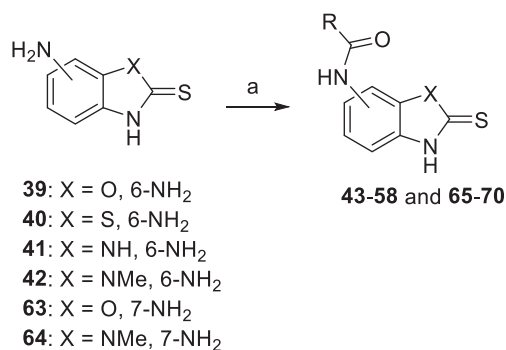
Due to the lack of clear SAR, we tried to obtain further evidence for the binding of these compounds to the $\beta 5i$ subunit. Therefore, we performed microscale thermophoresis experiments using the isolated $\beta 5i$ subunit. Compounds **36**, **43**, **44**, and **48** were shown to bind in single point measurements, and dissociation constants were determined for compounds **12**, **18**, and **47** from the 'thiazole' 'imidazole' and 'oxazole' series, respectively (Figure S3). These results confirmed the direct binding of selected compounds to the $\beta 5i$ subunit of iCP and quantified their binding by K_d values in the low-to-mid micromolar range.

To exclude the possibility that compounds are false positive hits, common liabilities causing false positives in biochemical screens [63] were addressed. We started with assays for potential redox activity of compounds using three different assays, each with a distinct mechanism, namely H₂O₂ generation, formation of reactive oxygen species (ROS), and free radicals. To evaluate the possibility that compounds generate H₂O₂ and cause non-specific inhibition, the horseradish peroxidase-phenol red (HRP-PR) assay was utilized. This assay is used to detect H₂O₂, generated by redox active compounds in the presence of dithiothreitol (DTT) or under redox-free conditions. Increase in absorbance is measured due to HRP catalyzed oxidation of phenol red with H₂O₂ at 610 nm [64]. None of the compounds was found to generate H₂O₂ (Table S3: HRP-PR assay). A cell-permeant fluorescent probe 2',7'-dichlorodihydrofluorescein diacetate (H₂DCFDA) was used to detect ROS formation [65]. Apart from compound **21**, none of the evaluated benzoXazole-2(3H)-thiones was found to form ROS in redox free conditions or in the presence of a reducing agent tris(2-carboxyethyl)phosphine (TCEP) (Table S3: H₂DCFDA assay). To evaluate the possibility that compounds caused enzyme inhibition through generation of free radicals, the resazurin assay was performed. Namely, redox active compounds convert resazurin to resorufin in the presence of DTT and a radical type of mechanism is proposed for this oxidation [66]. Again, using the resazurin assay we showed that benzoXazole-



Scheme 1. Synthesis of 1-methyl-6-nitro-1,3-dihydro-2H-benzo[d]imidazole-2-thione (**38**), 7-bromo-1-methyl-1,3-dihydro-2H-benzo[d]imidazole-2-thione (**60**), and various benzoXazole-amine derivatives (**42**, **63**, **64**)^a

^aReagents and conditions: (a) MeI, Na₂CO₃, DMF, rt, 16 h, 43%; (b) TCDI, THF, rt, 16 h, 90% for **38**, 69% for **60**, 72% for **V**, 54% for **64**; (c) H₂, 10% Pd/C, THF, rt, 16 h, 92%; (d) SnCl₂ × 2H₂O, DMF, 70 °C, 2 h, 61%; (e) H₂, 10% Pd/C, THF, rt, 2 h, 99%.



Scheme 2. Synthesis of 6- and 7-amide-substituted benzoXazole-2(3H)-thiones^a

^aReagents and conditions: (a) appropriate carboxylic anhydride, DMAP, Et₃N, DMF, rt, 16 h, 48% for **43**, 45% for **44**, 44% for **47**, 61% for **48**; or carboxylic acid, HATU, DMF, 50 °C, 24 h, 67% for **50**, 72% for **51**, 56% for **52**, 50% for **53**, 46% for **54**, 60% for **56**, 67% for **57**, 10% for **58**; or carboxylic acid, HATU, Et₃N, DMF, rt, 16 h, 33% for **46**, 34% for **49**, 27% for **55**, 54% for **65**, 47% for **66**, 51% for **67**, 22% for **68**, 33% for **69**, 43% for **70**.

2(3H)-thiones did not inhibit the β5i subunit of iCP *via* this non-specific mechanism (Table S3: Resazurin assay).

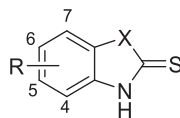
After testing for redox activity, several additional assays were performed to analyze potential chemical reactivity of benzoXazole-2(3H)-thiones. Firstly, an NMR-based assay was utilized to detect possible adducts with glutathione (GSH), which was incubated with selected compounds (**1**, **2**, **6**, **9**, and **13**; benzoisothiazolone was used as a positive control). No interaction with GSH was detected after 24 h (Figures S4–S9). Secondly, an HPLC-MS assay was used, where compounds **4**, **6–9**, **12**, **13**, **16–18**, **27**, **28**, and **37** were incubated with GSH at four different pH values: 7.4, 8.0, 8.5, 9.0 in phosphate buffered saline (PBS) buffer. Solutions were kept at 37 °C overnight and the following analysis with HPLC-MS revealed no adducts. Similarly, *N*-benzoylthreonine was used instead of GSH and incubated with compounds overnight at pH 9.0. Again, no adducts were detected (Table S4). Next, we utilized a high-throughput thiol reactivity assay with reduced 5,5'-dithiobis-(2-

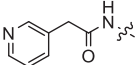
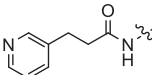
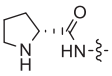
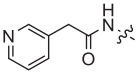
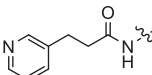
nitrobenzoic acid) (DTNB), where recently the rate of alkylation for a library of electrophilic fragments was determined by following the decrease in absorbance at 412 nm [67]. DTNB is first reduced to 5-mercapto-2-nitrobenzoic acid (TNB²⁻) with the addition of TCEP. The presence of a reducing agent allows the detection of nucleophilic addition or nucleophilic substitution but prevents the formation of disulfides, as DTNB itself is a disulfide. Unsurprisingly, none of the benzoXazole-2(3H)-thiones was found to be reactive in this assay (Table S3: High-throughput thiol reactivity assay).

Because our next aim was to detect the potential formation of disulfides, we further developed this assay (and called it the 'TNB²⁻ depletion' assay) by omitting TCEP from the procedure. Therefore, we used commercially available TNB²⁻ instead of DTNB. In a blank experiment, we found a higher baseline drift due to the formation of DTNB. This process slows down under argon atmosphere and is dependent on the presence of oxygen in solution (data not shown). Compounds were incubated with TNB²⁻ and in the case of reaction between the benzoXazole-2(3H)-thiones and TNB²⁻, a decrease in absorbance at 412 nm was observed (measured for up to 24 h). Formation of disulfides was confirmed by the addition of TCEP after 16 h, which transformed disulfides back to TNB²⁻ and free compounds resulting in the restoration of high absorbance for all benzoXazole-2(3H)-thiones (compounds **19**, **22**, **29**, and **36** as examples in Fig. 3). However, the absorbance for covalently bound control compound chloroacetamide remained unchanged after the addition of TCEP (Fig. 3). In general, approximately half of the benzoXazole-2(3H)-thiones was found to facilitate TNB²⁻ depletion and there was a clear correlation between the ability of compounds to deplete TNB²⁻ and their ability to inhibit β5i subunit of iCP (Table 3 and Table S3: TNB²⁻ depletion assay).

Next, we wanted to use NMR to confirm the formation of a mixed disulfide between TNB²⁻ and compound **29**. However, no mixed disulfide was detected by this method and the only observation was an accelerated formation of DTNB in the presence of compound **29** compared to blank control (Figure S10). Therefore, we proposed a mechanism where all reactions are reversible and in

Table 2
Inhibitory potencies of benzoXazole-2(3H)-thiones against the $\beta 5i$ subunit of human iCP.



R	X = O	X = S	X = NH ^d	X = NMe
	RA (%) at 100 μ M or IC ₅₀ (μ M) ^b	RA (%) at 100 μ M or IC ₅₀ (μ M) ^b	RA (%) at 10 μ M or IC ₅₀ (μ M) ^b	RA (%) at 100 μ M or IC ₅₀ (μ M) ^b
4-Me		19 , 19 \pm 4.0 μ M	20 , 84%	
4-OMe	21 , 81 \pm 5.0 μ M			
4-OH	22 , 4.1 \pm 0.9 μ M			
5-Me	23 , 99% ^c	24 , 56% ^c	- ^d	
5-OMe	25 , 59%	26 , 7.2 \pm 6.1 μ M	- ^d	
5-NO ₂	27 , 9.0 \pm 5.0 μ M	28 , 58%	- ^d	
6-Me	29 , 30 \pm 25 μ M	30 , 55% ^{c,e}	31 , 95%	
6-OMe		32 , 13 \pm 7.1 μ M	33 , 97%	
6-OEt		34 , 9.0 \pm 5.2 μ M	35 , 80%	
6-COOMe	36 , 3.0 \pm 1.3 μ M			
6-NO ₂		37 , 69% ^c		38 , 52%
6-NH ₂	39 , 21 \pm 27 μ M	40 , 80% ^c	41 , 49%	42 , 67%
6-NHCOMe	43 , 63%	44 , 130 \pm 43 μ M	45 , 97%	46 , 149 \pm 7.0 μ M
6-NHCOPh	47 , 49 \pm 3.2 μ M	48 , 7.1 \pm 6.0 μ M		49 , 39% ^e
position 6	50 , 50%	51 , 15 \pm 4.1 μ M		52 , 89%
				
position 6	53 , 56%	54 , 26 \pm 6.4 μ M		55 , 72%
				
position 6	56 , 65%	57 , 95 \pm 13 μ M		58 , 109 \pm 4.0 μ M
				
7-Br		59 , 11 \pm 1.3 μ M		60 , 87%
7-Ph		61 , 54% ^c		
position 7		62 , 70%		
				
7-NH ₂	63 , 79 \pm 2.2 μ M			64 , 63%
7-NHCOMe	65 , 129 \pm 22 μ M			66 , 47%
position 7	67 , 156 \pm 12 μ M			68 , 94%
				
position 7	69 , nd ^f			70 , 92%
				

^a Due to the plane of symmetry in benzo[d]imidazole-2(3H)-thiones, substitutions at positions 5 and 7 are equivalent to substitutions at positions 6 and 4, respectively.

^b RAs and IC₅₀ values are means from at least three independent determinations. Standard deviations for RAs are not included (for clarity) and were <20%.

^c RA value was determined at 10 μ M due to limited solubility of compounds in the assay buffer at 100 μ M.

^d Compound does not exist due to symmetry.

^e IC₅₀ could not be determined due to poor solubility in the assay buffer at higher concentrations.

^f Not determined due to poor solubility in DMSO.

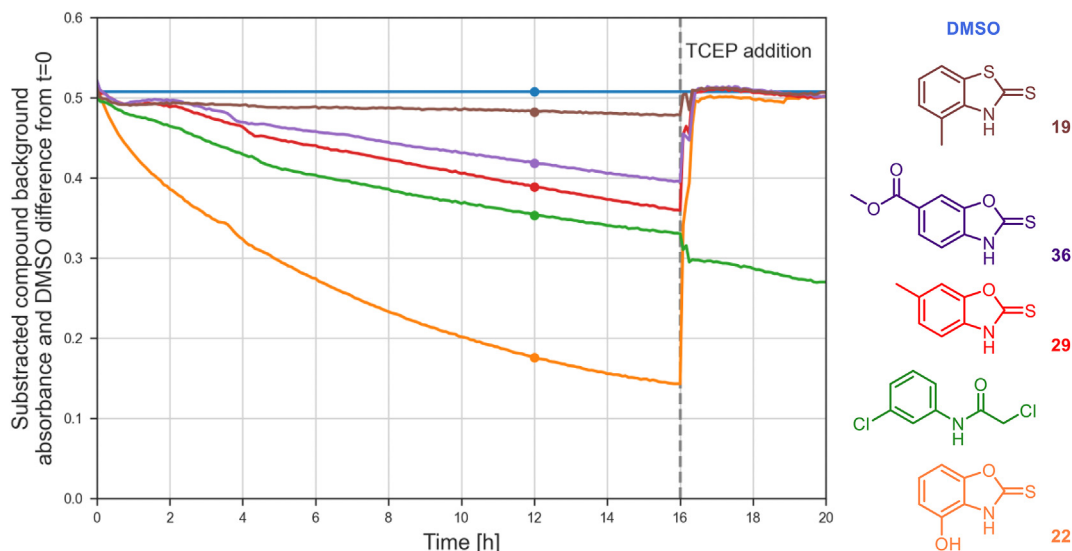


Fig. 3. Schematic representation of the “TNB²⁻ depletion assay” for **19**, **22**, **29**, **36**, and 2-chloro-*N*-(3-chlorophenyl)acetamide. Both baseline and compound background absorbance were subtracted in all cases. The dashed line denotes TCEP addition, which restores high absorbance only in the case of benzoXazole-2(3*H*)-thiones suggesting that mixed disulfides are transformed back to TNB²⁻ and benzoXazole-2(3*H*)-thione, whereas irreversibly covalently modified TNB²⁻ (such as alkylated into thioether with chloroacetamide) is not restored. The dots denote a time point ($t = 12$ h) used for reporting TNB²⁻ depletion in Table 3 and Table S3.

compounds **72** and **79**, a complete lack of concentration-dependence was observed resulting in our decision to discard compounds with these two warheads from further evaluation. 1,3-Benzothiazole-2-sulfonyl fluoride (**78**) inhibited $\beta 5i$ in a concentration-dependent manner with an IC_{50} value of $11 \pm 2.0 \mu M$ (Table 4, Figure S11). Despite showing preferential inhibition of $\beta 5i$ over the $\beta 5$ subunit (7-fold, Table 4, Figure S11), **78** inhibited other subunits of the iCP ($\beta 1i$, $\beta 2i$) and cCP ($\beta 2$) as well (Table S7). On the other hand, compound **75** showed a better selectivity profile as RA values remained above 80% for all subunits tested (Table S7). For these reasons and also due to better synthetic accessibility, 2-nitrile-substituted benzoXazoles were investigated further. Notably, compounds **75** and **78** retained inhibition also in the presence of 1 mM TCEP in the assay buffer (Table S7).

2.5. Chloro scan of carbonitriles

Similarly as before with benzoXazole-2(3*H*)-thiones, we decided to perform the chloro scan with benzoXazole-2-carbonitriles, where we mostly focused on positions 6 and 7 of the benzoXazole rings (Table 5). The selection of compounds was again done by scanning through commercially available chemical space (i.e. **83**, **86**, and **87**; characterized and described in the Supporting Information) and by synthetic approaches (Scheme 5).

Key reagents for the synthesis of chloro-substituted benzoXazole-2-carbonitriles **84**, **85**, and **88–92** (Scheme 5) were appropriate aniline derivatives **XIX–XXV** and 4,5-dichloro-1,2,3-dithiazolium chloride (Appel's salt). These reactions were performed in pyridine with varying reaction conditions depending on the aniline starting compound. Some of these (i.e. **XXI**, **XXIV**, and **XXV**) also had to be prepared synthetically. To provide **XXI**, 2,3-dichloroaniline (**XIV**) was first reacted with potassium ethyl xanthate to give 7-chlorobenzo[*d*]thiazole-2(3*H*)-thione (**12**). This was then heated in hydrazine hydrate at 110 °C to provide the desired thiole **XXI**. Because of *in situ* disulfide formation this compound was transferred to the next reaction immediately. To prepare 5-chloro- (**XXIV**) and 6-chloro-*N*¹-methylbenzene-1,2-diamine (**XXV**), corresponding 2-nitroaniline derivatives **XV** and **XVI**, respectively, were used as starting material. Both were initially

methylylated to yield compounds **XVII** and **XVIII** and then reduced using tin(II) chloride to give the desired diamines **XXIV** and **XXV** (Scheme 5).

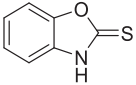
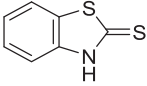
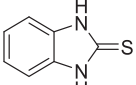
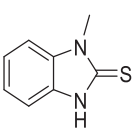
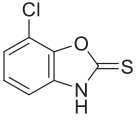
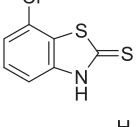
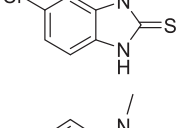
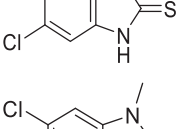
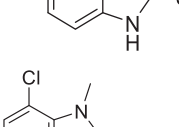
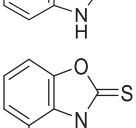
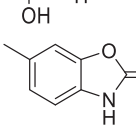
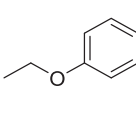
The addition of a chlorine atom at positions 6 and 7 in all cases led to improved $\beta 5i$ inhibition (compare for example data for non-substituted compounds **74**, **75**, **76**, and **77** [Table 4] to their 7-chloro-substituted counterparts **88**, **85**, **90**, and **92**, respectively [Table 5]). Besides the more than 8-fold better inhibition of $\beta 5i$ activity determined for these compounds, selectivity against $\beta 5$ subunit was retained. Compounds **88** and **92** were assayed also against other iCP and cCP subunits and in all cases RA values were above 82% demonstrating selective $\beta 5i$ inhibition for these fragment-like compounds (Table S7). In addition, we evaluated the ability of compounds **84**, **85**, **88**, and **92** to inhibit the $\beta 5i$ subunit of iCP in the presence of 1 mM TCEP (Table S7). We did observe approximately 3-fold decrease in their IC_{50} values and this can be attributed to the nucleophilic nature of TCEP, which can react with electrophiles, decreasing their actual concentration in the assay, as reported previously by several groups [71,72]. Interestingly, however, adding a chlorine onto the benzoXazole scaffold resulted in a positive high-throughput thiol reactivity assay only for the 1,3-benzoxazoles (compounds **83–85**, Table 5) and for the 7-substituted 1-methylbenzimidazole **92**.

IC_{50} shift experiments were also performed. A very marginal time-dependence was observed for the sulfonyl fluoride **78**. We also demonstrated a slightly time-dependent $\beta 5i$ inhibition for nitriles **75**, **84**, **85**, **88**, **89**, and **92** (Table S8, Figure S12), which could be indicative of a (reversible) covalent interaction between the electrophilic group at position 2 and the Cys48 in the active site of the $\beta 5i$ subunit.

We performed further studies with compound **84** to investigate its binding mode. MS/MS experiments showed that labelling by **84** yields approximately equal quantity of unlabelled and single labelled protein with a small amount of double labelled product (Figure S18). MS/MS identification of the labelling sites with digested protein was unsuccessful probably owing to the removal of the reversibly binding inhibitor under the conditions of digestion. Therefore, Ellman's assay for $\beta 5i$ with and without treatment by **84** was performed to assess the amount of cysteine labelling.

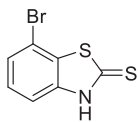
Table 3

Inhibitory potencies of selected compounds against the $\beta 5$ subunit of cCP. IC₅₀ values against the $\beta 5$ subunit of iCP are also shown to enable better comparison. The ability of compounds to deplete TNB²⁻ is shown as well, which suggests their ability to form mixed disulfides.

Compound	Structure	$\beta 5$ i RA (%) at 10 μ M or IC ₅₀ (μ M) ^a	$\beta 5$ RA (%) at 100 μ M ^a	TNB ²⁻ depletion ^b
1		17 ± 3.6 μ M	116%	yes
2		13 ± 4.1 μ M	85%	yes
3		114 ± 16 μ M	100%	no
4		94 ± 8.9 μ M	91%	no
8		16 ± 0.4 μ M	94%	yes
12		9.7 ± 1.9 μ M	59% ^c	yes
13		62 ± 7.8 μ M	98%	no
16		80% ^d	100%	no
17		4.2 ± 0.9 μ M	94%	yes
18		1.8 ± 0.3 μ M	99%	yes
22		4.1 ± 0.9 μ M	87%	yes
29		30 ± 25 μ M	92%	yes
35		80%	95%	no

(continued on next page)

Table 3 (continued)

Compound	Structure	$\beta 5i$ RA (%) at 10 μM or IC_{50} (μM) ^a	$\beta 5$ RA (%) at 100 μM ^a	TNB ²⁻ depletion ^b
59		11 \pm 1.3 μM	84%	yes

^a RAs and IC_{50} values are means from at least three independent determinations. Standard deviations for RAs are not included and were <20%.

^b TNB²⁻ depletion cutoff was greater than 3-fold the standard deviation over the DMSO blanks after 12 h. The concentration of compounds in this assay was 200 μM .

^c Approximate value due to poor solubility at 100 μM ^dRA determined at 150 μM of compound.

Considering that $\beta 5i$ has two solvent accessible cysteines, Cys48 and Cys88 (Table S9), and assuming that cysteine labelling was observed by MS/MS, the measured ~45% single labelled and ~10% double labelled protein corresponds to $(0.45 \times 1/2 + 0.10 \times 1) \sim 33\%$ labelling in the Ellman's assay. This number agrees well with $34.9 \pm 5.1\%$ cysteine labelling measured with Ellman's assay. An examination of the location of the accessible cysteines using the X-ray structure of $\beta 5i$ (PDB 6E5B) [55] reveals that while Cys48 is on the edge of the substrate binding channel, Cys88 is on the surface of the domain and its sulfur atom is separated by over 23 Å from the sidechain oxygen of the catalytic Thr1 residue. These findings additionally suggest that **84** exerts its inhibitory activity by reversible covalent binding to Cys48.

3. Conclusions

Here, we described selective fragment-sized inhibitors of the $\beta 5i$ subunit of iCP. Although benzoXazole-2(3H)-thione hits did selectively inhibit $\beta 5i$ activity, further mechanistic studies revealed an inhibition mechanism with limitations that could negatively affect their cellular activity. Thorough exploration of the available fragment space and the generated SAR provided valuable data that was exploited in subsequent design. Optimization of the warhead at position 2 resulted in biologically more relevant Cys-targeting moieties. This strategy eventually led to the discovery of 7-chloro-substituted benzoXazole-2-carbonitriles that inhibited the $\beta 5i$ subunit of iCP in the low micromolar range, showed preferential inhibition of $\beta 5i$ over $\beta 5$, and concurrently showed negligible

activity against the $\beta 1$ and $\beta 2$ subunits of both CPs. These results suggest that fragment based approaches – as the ‘five smooth stones’ of David against Goliath – can contribute to identify and develop non-peptide inhibitors against a fairly large and complex proteasome target. These viable chemical starting points might be suitable for further investigation and development of $\beta 5i$ -selective probes for non-cancer indications related to the iCP.

4. Experimental section

4.1. General chemistry methods

Reagents and solvents were obtained from commercial sources (Acros Organics, Aldrich, TCI Europe, Merck, Alfa Aesar, Fluorochem) and were used as received. DPLG-3 was synthesized as described previously [43,56]. PR-957 and carfilzomib were purchased from MedChemExpress. Compounds for assays were obtained from Enamine, Specs, Vitas-M, Maybridge, AK Scientific, BioNET, ArkPharm, Fluorochem, Combi-Blocks, Apollo Scientific, and Asta Tech). For reactions involving air or moisture sensitive reagents, solvents were distilled before use and these reactions were carried out under nitrogen or argon atmosphere. Reactions were monitored using analytical thin-layer chromatography plates (Merck 60 F254, 0.20 mm), and the components were visualized under UV light and/or through staining with the relevant reagent. Flash column chromatography was performed using a CombiFlash Rf 200 device (Teledyne ISCO, Lincoln, NE, USA) and in the case of reversed phase chromatography RediSep Rf Reversed-phase C18

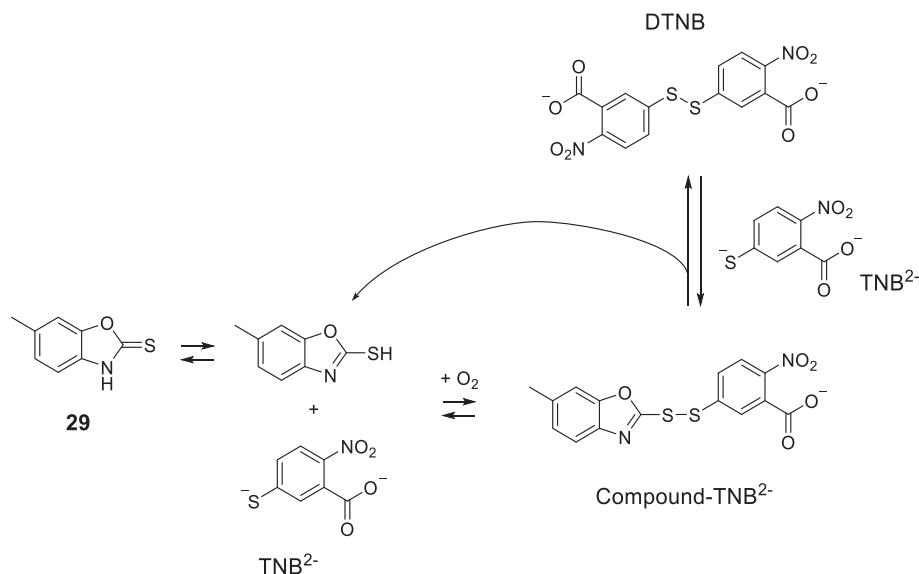
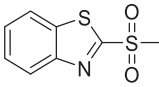
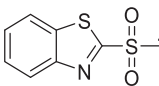
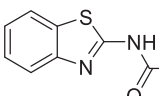
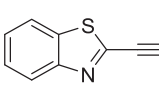
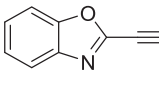
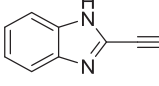
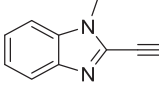
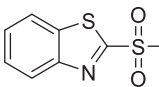
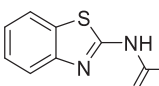
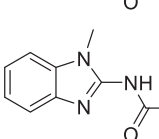


Fig. 4. Proposed mechanism of the reaction between compound **29** and TNB²⁻. Mixed disulfide (compound-TNB²⁻) was not detected in NMR but was detected in trace amounts in HRMS experiment. DTNB was detected both in NMR and HRMS as the major species.

Table 4

Inhibitory potencies of 2-substituted benzoXazoles against the $\beta 5i$ subunit of human iCP. Inhibitory potencies of selected compounds against the $\beta 5$ subunit of cCP and reactivity in the high-throughput thiol reactivity assay are also shown.

Compound	Structure	$\beta 5i$ RA (%) at 100 μM or IC_{50} (μM) ^a	$\beta 5$ RA (%) at 100 μM or IC_{50} (μM) ^a	High-throughput thiol reactivity ^b
71		88%	nd ^c	reactive
72		40% ^d	nd	highly reactive
73		73%	nd	highly reactive
74		61%	nd	not reactive
75		83 \pm 6.0 μM	82%	not reactive
76		89%	nd	not reactive
77		99% ^e	nd	not reactive
78		11 \pm 2.0 μM	81 \pm 4.1 μM	not reactive
79		44% ^d	nd	reactive
80		83%	nd	not reactive

^a RAs and IC_{50} values are means from at least three independent determinations. Standard deviations for RAs are not included and were <20%.

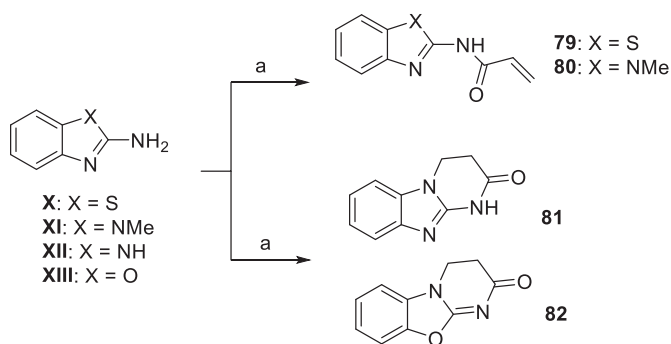
^b High-throughput thiol reactivity was determined after 4 h with threshold greater than 3-fold the standard deviation over the DMSO blanks. Compounds were labelled as highly reactive if the plateau was reached in the first 10 h.

^c Not determined.

^d For compounds **72** and **79**, IC_{50} was not determined due to lack of concentration dependence. Namely, **72** and **79** had the same percent of inhibition, i.e. 50–60%, regardless of the compound concentration used, i.e. from 25 μM to 250 μM ^eHigh background fluorescence.

columns were used. Normal phase flash column chromatography was performed on Merck Silica Gel 60 (particle size 0.040–0.063 mm; Merck, Germany). Melting points were determined on an OptiMelt SRS (Sunnyvale, CA, USA) and Reichelt hot-stage apparatus, and are uncorrected. ^1H and ^{13}C NMR spectra were recorded at 295 K on a Varian System 500 NMR spectrometer (Varian, Palo Alto, CA, USA), Varian System 300 NMR spectrometer or Bruker Avance III 400 MHz spectrometer (Bruker, Billerica, MA, USA) operating at frequencies for ^1H NMR at 500 MHz, 400 MHz or 300 MHz, and for ^{13}C NMR at 125 MHz, 101 MHz or 75 MHz. The chemical shifts (δ) are reported in parts per million (ppm) and are referenced to the deuterated solvent used. The coupling constants (J) are given in Hz, and the splitting patterns are designated as follows: s, singlet; br s, broad singlet; d, doublet; app d, apparent doublet; dd, double doublet; ddd, doublet of doublets of doublets; t, triplet; dt, doublet of triplets; td, triplet of doublets; m, multiplet.

All ^{13}C NMR spectra were proton decoupled. Mass spectra data and high-resolution mass measurements were performed on a Thermo Scientific Q Exactive Plus mass spectrometer (Thermo Fisher Scientific, Waltham, MA, USA) at the Faculty of Pharmacy, University of Ljubljana. Analytical reversed-phase HPLC for compounds used in biochemical assays (purchased and synthesized) was performed on Thermo Scientific Dionex UltiMate 3000 UHPLC modular system (Thermo Fisher Scientific, Waltham, MA, USA), equipped with a photodiode array detector set to 254 nm. An Acquity UPLC® BEH Phenyl Column (2.1 \times 100 mm; 1.7 μm) was used, it was thermostated at 40 $^\circ\text{C}$, and flow rate was set to 0.3 mL/min 1 μL of 0.05 mg/mL sample solution was injected. An eluent system of A (0.1% TFA in H_2O) and B (MeCN) was used with gradient elution: 0–9 min, 5% B \rightarrow 80% B; 9–11 min, 80% B; 11–11.5 min, 80% B \rightarrow 5% B. The purities of the test compounds used for the biological evaluations were $\geq 95\%$, unless stated otherwise. HPLC-MS measurements were

**Scheme 4.** Synthesis of acrylamide-based derivatives^d

^dReagents and conditions: (a) acryloyl chloride, Et₃N, THF, 0 °C, 30 min, rt, overnight (15% for **79** and 13% for **80**) or 1 h (24% for **81** and 14% for **82**).

performed using a Shimadzu LC-MS-2020 device (Shimadzu Corporation, Kyoto, Japan) equipped with a Reprospher 100 C18 (5 μm, 100 × 3 mm) column and positive-negative double ion source (DUIS±) with a quadrupole mass spectrometer in a range of 50–1000 *m/z*. Sample was eluted with gradient elution using eluent A (0.1% HCOOH in H₂O) and eluent B (0.1% HCOOH in CH₃CN). Flow rate was set to 1.5 mL/min. The initial condition was 0% B eluent, followed by a linear gradient to 100% B eluent by 2 min, from 2 to 3.75 min 100% B eluent was retained, and from 3.75 to 4.5 min back to initial condition and retained to 5 min. The column temperature was kept at 30 °C and the injection volume was 1 μL.

4.1.1. General acylation procedures

General acylation procedure 1. To a solution of the appropriate amine (1.0 equiv.) in DMF (0.5 mL), HATU (1.5 equiv.) and the corresponding carboxylic acid (1.5 equiv.) were added and the reaction

Table 5

Inhibitory potencies of chloro-substituted benzoXazole-2-carbonitriles against the β5i subunit of human iCP. Inhibitory potencies of selected compounds against the β5 subunit of cCP and reactivity in the high-throughput thiol reactivity assay are also shown.

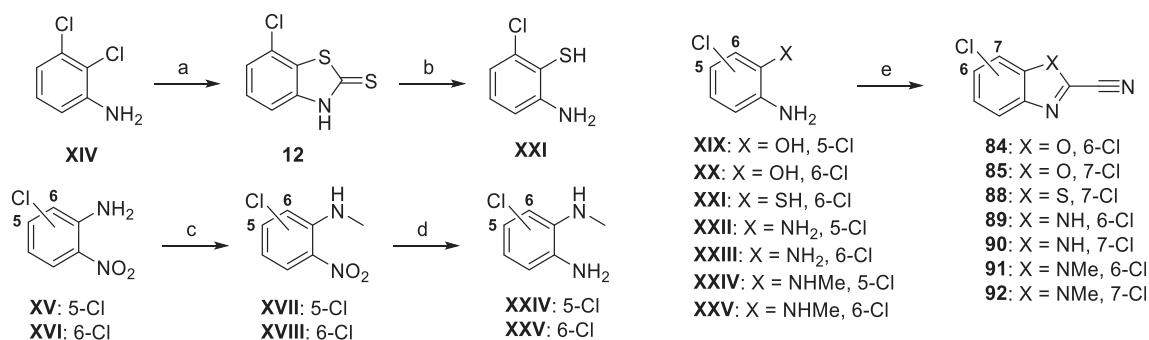
Compound	Structure	β5i RA (%) at 100 μM or IC ₅₀ (μM) ^a	β5 RA (%) at 100 μM or IC ₅₀ (μM) ^a	High-throughput thiol reactivity ^b
83		67 ± 11 μM	101%	reactive
84		9.1 ± 4.5 μM ^c	45 ± 17 μM ^c	reactive
85		10 ± 4.6 μM ^c	93 ± 34 μM ^c	highly reactive
86		85 ± 10 μM	nd ^d	not reactive
87		58%	nd	not reactive
88		18 ± 4.9 μM	72%	not reactive
89		28 ± 3.1 μM	71%	not reactive
90		75 ± 24 μM	82%	not reactive
91		50%	nd	not reactive
92		20 ± 9.3 μM	89%	reactive

^a RAs and IC₅₀ values are means from at least three independent determinations. Standard deviations for RAs are not included and were <20%.

^b High-throughput thiol reactivity was determined after 4 h with threshold greater than 3-fold the standard deviation over the DMSO blanks. Compounds were labelled as highly reactive if the plateau was reached in the first 10 h.

^c Inhibition of iCP and cCP activities determined with the use of alternative substrate (Suc-LLVY)₂R110, because of compounds' autofluorescence and interference with AMC-based substrate.

^d Not determined.



Scheme 5. Synthesis of anilines **XXI**, **XXIV**, **XXV** and benzoXazole-2-carbonitriles **84**, **85**, and **88–92**^a

^aReagents and conditions: (a) potassium ethyl xanthate, DMF, 140 °C, 3 h, 80%; (b) hydrazine hydrate, 110 °C, 16 h, 30%; (c) 1. NaH, THF, 0 °C, 15 min; 2. MeI, rt, 2 h (95% for **XVII**) or 50 °C, 16 h (44% for **XVIII**); (d) SnCl₂ × 2H₂O, EtOAc, reflux, 16 h, 88% for **XXIV**, 25% for **XXV**; (e) Appel's salt, pyridine, for specific conditions, see Experimental section, 24% for **84**, 17% for **85**, 30% for **88**, 56% for **89**, 56% for **90**, 53% for **91**, 26% for **92**.

mixture was stirred at 50 °C for 16 h. After the reaction was complete, the crude product was purified by reversed phase flash column chromatography using CH₃CN:H₂O as an eluent system (gradient from 1:9 to 10:0).

General acylation procedure 2. In a vial, to the solution of the appropriate amine in DMF (0.5 mL), HATU (1.2 eq), Et₃N (1.2 equiv. or 2.2 equiv. in the case of hydrochloric salts on pyridine derivatives), and the corresponding carboxylic acid (1.2 equiv.) were added and reacted at room temperature for 16 h. After the reaction was complete, the crude product was purified by reversed phase flash column chromatography using CH₃CN:H₂O as an eluent system (gradient from 1:9 to 10:0).

General acylation procedure 3. To a solution of the appropriate amine (1.0 equiv.) in DMF (5 mL), Et₃N (3 equiv.), *N,N*-dimethylaminopyridine (0.1 equiv.) and the corresponding acid anhydride (3 equiv.) were added and the mixture was stirred for 16 h. The reaction was quenched with H₂O (20 mL) and washed with EtOAc (3 × 20 mL). The organic phases were collected, dried with MgSO₄, filtered and the solvent was evaporated to yield final compounds.

4.2. Procedure for the preparation of compounds 38 and 42. To a solution of 4-nitrobenzene-1,2-diamine (**I**, 5.00 g, 32.65 mmol, 1.25 equiv.) in DMF (75 mL), Na₂CO₃ (1.73 g, 16.32 mmol, 0.625 equiv.) was added, followed by a dropwise addition of MeI (1.63 mL, 26.12 mmol, 1.0 equiv.). The mixture was allowed to stir at room temperature for 16 h. Then it was concentrated and subjected to flash column chromatography using EtOAc:*n*-hexane (7:3) as an eluent system. The product, *N*¹-methyl-5-nitrobenzene-1,2-diamine (**II**), was obtained as a yellow solid (2.34 g, 43% yield). Physical and spectroscopic data were identical to those reported previously [73].

Compound **II** (2.60 g, 15.57 mmol, 1.0 equiv.) was dissolved in THF (60 mL) and TCDI (3.05 g, 17.13 mmol, 1.1 equiv.) was added. The solution was stirred at room temperature for 16 h. Then, the mixture was concentrated and the residue dissolved in DMF (16 mL). H₂O (60 mL) was subsequently added and the pH was adjusted to 1 with the addition of 1 M HCl. The mixture was allowed to stand for 4 h. The precipitate was filtered, washed with H₂O (2 × 50 mL), and dried to obtain 1-methyl-6-nitro-1,3-dihydro-2*H*-benzo[d]imidazole-2-thione (**38**) as a yellow solid (2.95 g, 90% yield). Mp.: 260 °C; ¹H NMR (500 MHz, DMSO-*d*₆) δ 13.27 (s, 1H), 8.24 (d, *J* = 2.1 Hz, 1H), 8.08 (dd, *J* = 8.7, 2.1 Hz, 1H), 7.29 (d, *J* = 8.7 Hz, 1H), 3.70 (s, 3H); ¹³C NMR (126 MHz, DMSO-*d*₆) δ 171.90, 142.57, 135.73, 133.16, 119.24, 109.21, 105.24, 30.41; HRMS (APCI⁺) *m/z* [M+H]⁺, calcd. for C₈H₈N₃O₂S: 210.0337, found: 210.0334; Purity by HPLC: 99%.

To a solution of compound **38** (1.26 g, 6.0 mmol) in THF (30 mL), 10% Pd/C (Selcat Q6, 1.50 g) was added. The reactor was filled with

H₂ (8 bar) and the mixture was allowed to stir at room temperature for 16 h. It was then filtered through a pad of Celite, washed with THF (2 × 20 mL) and the volatiles evaporated. The product, 6-amino-1-methyl-1,3-dihydro-2*H*-benzo[d]imidazole-2-thione (**42**), was obtained as a brown solid (0.99 g, 92% yield). Mp.: 118 °C; ¹H NMR (500 MHz, DMSO-*d*₆) δ 12.28 (s, 1H), 6.89–6.85 (m, 1H), 6.47 (dd, *J* = 6.3, 2.0 Hz, 2H), 5.03 (s, 2H), 3.53 (s, 3H); ¹³C NMR (126 MHz, DMSO-*d*₆) δ 166.51, 145.02, 134.21, 121.90, 110.29, 110.06, 94.11, 29.73; HRMS (APCI⁺) *m/z* [M+H]⁺, calcd. for C₈H₁₀N₃S: 180.0595, found: 180.0593; Purity by HPLC: 99%.

4.3. Procedure for the synthesis of 7-bromo-1-methyl-1,3-dihydro-2*H*-benzo[d]imidazole-2-thione (60)

To a solution of 6-bromo-*N*¹-methylbenzene-1,2-diamine (**III**, 875 mg, 4.35 mmol, 1.0 equiv.) in THF (20 mL), TCDI (892 mg, 5.00 mmol, 1.15 equiv.) was added and the solution was stirred at room temperature for 16 h. The mixture was then concentrated and subjected to reversed phase flash column chromatography using eluents A (0.1% HCOOH in MeCN) and B (0.1% HCOOH in H₂O) (gradient from 1:9 to 10:0). Compound **60** was obtained as a light brown solid (731 mg, 69% yield). Mp.: 255 °C; ¹H NMR (500 MHz, DMSO-*d*₆) δ 13.02 (s, 1H), 7.35–7.32 (m, 1H), 7.17 (dd, *J* = 7.9, 0.7 Hz, 1H), 7.07 (t, *J* = 7.9 Hz, 1H), 3.97 (s, 3H); ¹³C NMR (126 MHz, DMSO-*d*₆) δ 170.02, 132.85, 130.15, 126.86, 124.27, 109.23, 101.72, 32.68; HRMS (APCI⁺) *m/z* [M+H]⁺, calcd. for C₈H₈BrN₃S: 242.9591 and 244.9571, found: 242.9591 and 244.9567; Purity by HPLC: 100%.

4.4. Procedure for the preparation of compound 63

To a solution of 2-amino-6-nitrophenol (**IV**, 311 mg, 2.02 mmol, 1.0 equiv.) in THF (20 mL), TCDI (396 mg, 2.22 mmol, 1.1 equiv.) was added and the solution was stirred at room temperature for 16 h. Then, the mixture was concentrated and the residue dissolved in DMF (8 mL). H₂O (30 mL) was subsequently added and the pH was adjusted to 1 with the addition of 1 M HCl. The mixture was allowed to stand for 4 h. The precipitate was then filtered and dried to obtain 7-nitrobenzo[d]oxazole-2(3*H*)-thione (**V**, 285 mg, 72% yield) as brown needles. Physical and spectroscopic data were identical to those reported previously [74].

To a solution of **V** (265 mg, 1.35 mmol, 1.0 equiv.) in DMF (10 mL), SnCl₂ × 2H₂O (1.828 g, 8.10 mmol, 6.0 equiv.) was added. The reaction was allowed to proceed at 70 °C for 2 h. After the reaction was complete, the mixture was concentrated and dissolved in EtOAc (60 mL), washed with saturated aqueous NaHCO₃ (2 × 60 mL) and brine (20 mL), dried with MgSO₄, and evaporated

to yield 7-aminobenzo[d]oxazole-2(3*H*)-thione (**63**, 137 mg, 61% yield) as a brown solid. Mp.: 202 °C; ¹H NMR (300 MHz, DMSO-*d*₆) δ 13.54 (s, 1H), 6.96 (t, *J* = 7.9 Hz, 1H), 6.51 (d, *J* = 8.1 Hz, 1H), 6.38 (d, *J* = 7.7 Hz, 1H), 5.65 (s, 2H); ¹³C NMR (75 MHz, DMSO-*d*₆) δ 179.44, 135.75, 132.50, 131.66, 125.72, 109.73, 97.44; HRMS (ESI⁺) *m/z* [M+H]⁺, calcd. for C₇H₇N₂O₂S: 167.0279, found: 167.0283; Purity by HPLC: 100%.

4.5. Procedure for the preparation of compound 64

To a solution of *N*-methyl-2,6-dinitroaniline (**VI**, 791 mg, 4.01 mmol) in THF (20 mL), 10% Pd/C (Selcat Q6, 150 mg) was added. The reactor was filled with H₂ (9.5 bar) and the mixture was allowed to stir at room temperature for 2 h. It was then filtered through a pad of Celite and concentrated. The product, *N*²-methylbenzene-1,2,3-triamine (**VII**), was obtained as a brown oil (543 mg, 99% yield). Physical and spectroscopic data were identical to those reported previously [75].

Compound **VII** (543 mg, 3.96 mmol, 1.0 equiv.) was dissolved in THF (55 mL) and TCDI (776 mg, 4.36 mmol, 1.1 equiv.) was added. The solution was stirred at room temperature for 16 h. Then, the mixture was concentrated and subjected to flash column chromatography using EtOAc:*n*-hexane (2:3) as an eluent system. The product, 7-amino-1-methyl-1,3-dihydro-2*H*-benzo[d]imidazole-2-thione (**64**), was obtained as a white solid (383 mg, 54% yield). Mp. 172 °C; ¹H NMR (500 MHz, DMSO-*d*₆) δ 12.43 (s, 1H), 6.86 (t, *J* = 7.9 Hz, 1H), 6.51–6.45 (m, 2H), 5.16 (s, 2H), 3.93 (s, 3H); ¹³C NMR (126 MHz, DMSO-*d*₆) δ 167.17, 133.79, 131.92, 123.64, 121.39, 110.20, 99.31, 32.45; HRMS (APCI⁺) *m/z* [M+H]⁺, calcd. for C₈H₁₀N₃S: 180.0595, found: 180.0593; Purity by HPLC: 99%.

4.6. Preparation of 6-(acylamino)benzo[d]oxazole-2(3*H*)-thione derivatives 43, 47, 50, 53, and 56

***N*-(2-thioxo-2,3-dihydrobenzo[d]oxazol-6-yl)acetamide (43)**. The reaction was carried out according to the General acylation procedure 3, starting from 6-aminobenzo[d]oxazole-2(3*H*)-thione (**39**, 50 mg, 0.3 mmol), Et₃N (125 μL, 0.9 mmol), *N,N*-dimethylaminopyridine (3 mg, 0.03 mmol), and acetic anhydride (85 μL, 0.9 mmol) to give compound **43** (30 mg, 48% yield) as a white solid. Mp.: 231 °C; ¹H NMR (300 MHz, DMSO-*d*₆) δ 13.46 (s, 1H), 10.13 (s, 1H), 7.88 (s, 1H), 7.35 (d, *J* = 8.4 Hz, 1H), 7.17 (d, *J* = 8.4 Hz, 1H), 2.06 (s, 3H); ¹³C NMR (75 MHz, DMSO-*d*₆) δ 179.82, 168.37, 148.17, 135.96, 126.51, 116.03, 110.32, 101.04, 23.97; HRMS (APCI⁺) *m/z* [M+H]⁺, calcd. for C₉H₉N₂O₂S: 209.0384, found: 209.0371; Purity by HPLC: 97%.

***N*-(2-thioxo-2,3-dihydrobenzo[d]oxazol-6-yl)benzamide (47)**. The reaction was carried out according to the General acylation procedure 3, starting from 6-aminobenzo[d]oxazole-2(3*H*)-thione (**39**, 50 mg, 0.3 mmol), Et₃N (125 μL, 0.9 mmol), *N,N*-dimethylaminopyridine (3 mg, 0.03 mmol), and benzoic anhydride (204 mg, 0.9 mmol) to give compound **47** (36 mg, 44% yield) as a white solid. Mp.: 238 °C; ¹H NMR (300 MHz, DMSO-*d*₆) δ 10.42 (s, 1H), 8.04 (d, *J* = 1.2 Hz, 1H), 7.97 (s, 1H), 7.95 (s, 1H), 7.66–7.50 (m, 4H), 7.23 (d, *J* = 8.5 Hz, 1H); ¹³C NMR (75 MHz, DMSO-*d*₆) δ 180.09, 165.58, 148.20, 135.59, 134.69, 131.68, 128.41, 127.69, 127.63, 117.39, 110.31, 102.29; HRMS (APCI⁺) *m/z* [M+H]⁺, calcd. for C₁₄H₁₁N₂O₂S: 271.0541, found: 271.0533; Purity by HPLC: 98%.

6-[2-(Pyridin-3-yl)acetamido]benzo[d]oxazole-2(3*H*)-thione (50). The reaction was carried out according to the General acylation procedure 1, starting from 6-aminobenzo[d]oxazole-2(3*H*)-thione (**39**, 40 mg (0.24 mmol), HATU (137 mg, 0.36 mmol), and 2-(pyridin-3-yl)acetic acid hydrochloride (62 mg, 0.36 mmol) to give compound **50** (46 mg, 67% yield) as a white solid. Mp.: 157–160 °C; ¹H NMR (300 MHz, DMSO-*d*₆) δ 13.82 (s, 1H), 10.53 (s, 1H), 8.82 (s,

1H), 8.77 (s, 1H), 8.35 (d, *J* = 7.9 Hz, 1H), 7.89 (t, *J* = 4.6 Hz, 2H), 7.37 (dd, *J* = 8.6, 1.9 Hz, 1H), 7.21 (d, *J* = 8.5 Hz, 1H), 3.95 (s, 2H); ¹³C NMR (75 MHz, DMSO-*d*₆) δ 179.97, 167.66, 148.13, 144.61, 144.56, 142.35, 135.47, 134.46, 126.87, 125.76, 116.30, 110.45, 101.30, 38.24; HRMS (ESI⁺) *m/z* [M+H]⁺, calcd. for C₁₄H₁₂N₃O₂S: 286.0650, found: 286.0651; Purity by HPLC: 100%.

6-[3-(Pyridin-3-yl)propanamido]benzo[d]oxazole-2(3*H*)-thione (53). The reaction was carried out according to the General acylation procedure 1, starting from 6-aminobenzo[d]oxazole-2(3*H*)-thione (**39**, 40 mg, 0.24 mmol), HATU (137 mg, 0.36 mmol), and 3-(pyridin-3-yl)propanoic acid (62 mg, 0.36 mmol) to give compound **53** (36 mg, 50% yield) as a white solid. Mp.: 274–276 °C; ¹H NMR (500 MHz, DMSO-*d*₆) δ 13.76 (s, 1H), 10.15 (s, 1H), 8.70 (s, 1H), 8.62 (d, *J* = 5.3 Hz, 1H), 8.16 (d, *J* = 8.1 Hz, 1H), 7.86 (d, *J* = 1.9 Hz, 1H), 7.71 (t, *J* = 6.8 Hz, 1H), 7.33 (dd, *J* = 8.5, 1.9 Hz, 1H), 7.17 (d, *J* = 8.5 Hz, 1H), 3.05 (t, *J* = 7.4 Hz, 2H), 2.74 (t, *J* = 7.3 Hz, 2H); ¹³C NMR (126 MHz, DMSO-*d*₆) δ 180.03, 170.05, 148.22, 144.54, 142.61, 142.46, 135.64, 126.75, 125.64, 116.35, 110.45, 101.35, 36.60, 27.54; HRMS (ESI⁺) *m/z* [M+H]⁺, calcd. for C₁₅H₁₄N₃O₂S: 300.0806, found: 300.0810; Purity by HPLC: 98%.

6-[(*R*)-pyrrolidine-2-carboxamido]benzo[d]oxazole-2(3*H*)-thione (56). The reaction was carried out according to the General acylation procedure 1, starting from 6-aminobenzo[d]oxazole-2(3*H*)-thione (**39**, 40 mg, 0.24 mmol), HATU (137 mg, 0.361 mmol), and (*R*)-pyrrolidine-2-carboxylic acid (41 mg, 0.36 mmol) to give compound **56** (38 mg, 60% yield) as a white solid. Mp.: 106–108 °C; ¹H NMR (500 MHz, DMSO-*d*₆) δ 10.65 (s, 1H), 7.84 (d, *J* = 1.8 Hz, 1H), 7.36 (dd, *J* = 8.5, 1.9 Hz, 1H), 7.22 (d, *J* = 8.5 Hz, 1H), 4.30 (dd, *J* = 8.4, 6.8 Hz, 1H), 3.30–3.23 (m, 4H), 1.95 (q, *J* = 7.0, 6.5 Hz, 2H); ¹³C NMR (126 MHz, DMSO-*d*₆) δ 180.33, 167.00, 148.39, 133.98, 116.36, 110.83, 101.46, 59.82, 45.89, 38.20, 29.50, 23.60; HRMS (ESI⁺) *m/z* [M+H]⁺, calcd. for C₁₂H₁₄N₃O₂S: 264.0806, found: 264.0804; Purity by HPLC: 100%.

4.7. Preparation of 6-(acylamino)benzo[d]thiazole-2(3*H*)-thione derivatives 44, 48, 51, 54, and 57

***N*-(2-thioxo-2,3-dihydrobenzo[d]thiazol-6-yl)acetamide (44)**. The reaction was carried out according to the General acylation procedure 3, starting from 6-aminobenzo[d]thiazole-2(3*H*)-thione (**40**, 55 mg, 0.3 mmol), Et₃N (125 μL, 0.9 mmol), *N,N*-dimethylaminopyridine (3 mg, 0.03 mmol), and acetic anhydride (85 μL, 0.9 mmol) to give compound **44** (30 mg, 45% yield) as a white solid. Mp.: 229 °C; ¹H NMR (300 MHz, DMSO-*d*₆) δ 13.74 (s, 1H), 10.32 (s, 1H), 8.05 (s, 1H), 7.49 (d, *J* = 8.4 Hz, 1H), 7.26 (d, *J* = 8.6 Hz, 1H), 2.05 (s, 3H); ¹³C NMR (75 MHz, DMSO-*d*₆) δ 188.72, 168.36, 136.84, 136.19, 129.74, 118.65, 112.46, 111.50, 23.90; HRMS (APCI⁺) *m/z* [M+H]⁺, calcd. for C₉H₉N₂O₂S: 225.0156, found: 225.0141; Purity by HPLC: 99%.

***N*-(2-thioxo-2,3-dihydrobenzo[d]thiazol-6-yl)benzamide (48)**. The reaction was carried out according to the General acylation procedure 3, starting from 6-aminobenzo[d]thiazole-2(3*H*)-thione (**40**, 55 mg, 0.3 mmol), Et₃N (125 μL, 0.9 mmol), *N,N*-dimethylaminopyridine (3 mg, 0.03 mmol), and benzoic anhydride (204 mg, 0.9 mmol) to give compound **48** (52 mg, 61% yield) as a white solid; Mp.: 209 °C; ¹H NMR (500 MHz, DMSO-*d*₆) δ 13.70 (s, 1H), 10.40 (s, 1H), 8.19 (s, 1H), 7.96 (d, *J* = 7.2 Hz, 2H), 7.70 (d, *J* = 8.4 Hz, 1H), 7.60 (t, *J* = 7.3 Hz, 1H), 7.54 (t, *J* = 7.4 Hz, 2H), 7.30 (d, *J* = 8.6 Hz, 1H); ¹³C NMR (126 MHz, DMSO-*d*₆) δ 189.07, 165.50, 137.36, 135.86, 134.64, 131.61, 129.65, 128.35, 127.59, 120.16, 113.09, 112.28; HRMS (APCI⁺) *m/z* [M+H]⁺, calcd. for C₁₄H₁₁N₂O₂S: 255.0593, found: 255.0578; Purity by HPLC: 99%.

6-[2-(Pyridin-3-yl)acetamido]benzo[d]thiazole-2(3*H*)-thione (51). The reaction was carried out according to the General acylation procedure 1, starting from 6-aminobenzo[d]thiazole-2(3*H*)-

thione (**40**, 100 mg, 0.55 mmol), HATU (343 mg, 0.82 mmol), and 2-(pyridin-3-yl)acetic acid hydrochloride (155 mg, 0.82 mmol) to give compound **51** (119 mg, 72% yield) as a white solid. Mp.: 127–130 °C; ¹H NMR (500 MHz, DMSO-*d*₆) δ 13.66 (s, 1H), 10.41 (s, 1H), 8.64 (s, 1H), 8.58 (d, *J* = 5.1 Hz, 1H), 8.01 (d, *J* = 2.0 Hz, 1H), 7.99 (d, *J* = 7.7 Hz, 1H), 7.58 (dd, *J* = 7.9, 5.1 Hz, 1H), 7.49 (dd, *J* = 8.7, 2.1 Hz, 1H), 7.25 (d, *J* = 8.7 Hz, 1H), 3.80 (s, 2H); ¹³C NMR (126 MHz, DMSO-*d*₆) δ 189.03, 168.01, 147.02, 144.82, 140.93, 137.18, 135.67, 129.87, 124.65, 118.99, 112.50, 111.98, 39.64; HRMS (ESI⁺) *m/z* [M+H]⁺, calcd. for C₁₄H₁₂N₃O₂S₂: 302.0422, found: 302.0416 Purity by HPLC: 99.0%.

6-[3-(Pyridin-3-yl)propanamido]benzo[d]thiazole-2(3H)-thione (54). The reaction was carried out according to the General acylation procedure 1, starting from 6-aminobenzo[d]thiazole-2(3H)-thione (**40**, 100 mg, 0.55 mmol), HATU (343 mg, 0.82 mmol), and 3-(pyridin-3-yl)propanoic acid (155 mg, 0.82 mmol) to give compound **54** (80 mg, 46% yield) as a white solid. Mp.: 119–121 °C; ¹H NMR (500 MHz, DMSO-*d*₆) δ 13.64 (s, 1H), 10.10 (s, 1H), 8.69 (s, 1H), 8.61 (s, 1H), 8.13 (dt, *J* = 8.1, 1.6 Hz, 1H), 8.00 (d, *J* = 2.0 Hz, 1H), 7.69 (dd, *J* = 7.9, 5.2 Hz, 1H), 7.42 (dd, *J* = 8.7, 2.1 Hz, 1H), 7.23 (d, *J* = 8.7 Hz, 1H), 3.04 (t, *J* = 7.3 Hz, 2H), 2.74 (t, *J* = 7.4 Hz, 2H); ¹³C NMR (126 MHz, DMSO-*d*₆) δ 188.99, 169.89, 144.79, 142.81, 141.99, 139.38, 137.03, 135.78, 129.88, 125.44, 118.89, 112.51, 111.84, 36.55, 27.55; HRMS (ESI⁺) *m/z* [M+H]⁺, calcd. for C₁₂H₁₄N₃O₂S₂: 316.0578, found: 316.0573; Purity by HPLC: 99%.

6-[(R)-pyrrolidine-2-carboxamido]benzo[d]thiazole-2(3H)-thione (57). The reaction was carried out according to the General acylation procedure 1, starting from 6-aminobenzo[d]thiazole-2(3H)-thione (**40**, 100 mg, 0.55 mmol), HATU (343 mg, 0.82 mmol), and (R)-pyrrolidine-2-carboxylic acid (103 mg, 0.82 mmol) to give compound **57** (103 mg, 67% yield) as a white solid. Mp.: 138–140 °C; ¹H NMR (500 MHz, DMSO-*d*₆) δ 10.61 (s, 1H), 7.99 (s, 1H), 7.50 (dd, *J* = 8.7, 1.9 Hz, 1H), 7.31 (d, *J* = 8.7 Hz, 1H), 4.31 (t, *J* = 7.4 Hz, 1H), 3.35–3.19 (m, 2H), 2.68 (s, 1H), 2.43–2.33 (m, 1H), 2.03–1.89 (m, 3H), resonance for NH missing; ¹³C NMR (126 MHz, DMSO-*d*₆) δ 189.33, 166.81, 137.86, 134.62, 130.07, 119.35, 112.69, 112.51, 59.83, 45.92, 29.51, 23.49; HRMS (ESI⁺) *m/z* [M+H]⁺, calcd. for C₁₂H₁₄N₃O₂S₂: 280.0578, found: 280.0574; Purity by HPLC: 100%.

4.8. Preparation of 6-(acylamino)-1-methylbenzo[d]imidazole-2(3H)-thione derivatives 46, 49, 52, 55, and 58

N-(3-methyl-2-thioxo-2,3-dihydro-1H-benzo[d]imidazole-5-yl)acetamide (46). The reaction was carried out according to the General acylation procedure 2, starting from 6-amino-1-methyl-1,3-dihydro-2H-benzo[d]imidazole-2-thione (**42**, 54 mg, 0.30 mmol), HATU (136 mg, 0.36 mmol), acetic acid (17 μL, 0.36 mmol), and Et₃N (50 μL, 0.36 mmol) to give compound **45** (22 mg, 33% yield) as a white solid. Mp.: 185 °C; ¹H NMR (500 MHz, DMSO-*d*₆) δ 12.63 (s, 1H), 10.00 (s, 1H), 7.75 (s, 1H), 7.22 (dd, *J* = 8.5, 1.3 Hz, 1H), 7.10 (d, *J* = 8.5 Hz, 1H), 3.60 (s, 3H), 2.05 (s, 3H); ¹³C NMR (126 MHz, DMSO-*d*₆) δ 168.47, 168.10, 134.73, 133.08, 126.48, 114.58, 109.51, 100.33, 29.88, 23.95; HRMS (ESI⁺) *m/z* [M+H]⁺, calcd. for C₁₀H₁₂N₃O₂S: 222.0701, found: 222.0702; Purity by HPLC: 100%.

N-(3-methyl-2-thioxo-2,3-dihydro-1H-benzo[d]imidazole-5-yl)benzamide (49). The reaction was carried out according to the General acylation procedure 2, starting from 6-amino-1-methyl-1,3-dihydro-2H-benzo[d]imidazole-2-thione (**42**, 54 mg, 0.30 mmol), HATU (136 mg, 0.36 mmol), benzoic acid (44 mg, 0.36 mmol), and Et₃N (50 μL, 0.36 mmol) to give compound **49** (29 mg, 34% yield) as a white solid. Mp.: 265 °C; ¹H NMR (500 MHz, DMSO-*d*₆) δ 12.69 (s, 1H), 10.30 (s, 1H), 8.02–7.89 (m, 3H), 7.62–7.49 (m, 4H), 7.17 (d, *J* = 8.4 Hz, 1H), 3.64 (s, 3H); ¹³C NMR (126 MHz, DMSO-*d*₆) δ 168.67, 165.36, 134.86, 134.43, 133.05, 131.46, 128.33, 127.53, 127.02, 116.02, 109.35, 101.75, 29.90; HRMS (APCI⁺) *m/z*

[M+H]⁺, calcd. for C₁₅H₁₄N₃O₂S: 284.0857, found: 284.0859; Purity by HPLC: 100%.

N-(3-methyl-2-thioxo-2,3-dihydro-1H-benzo[d]imidazole-5-yl)-2-(pyridin-3-yl)acetamide (52). The reaction was carried out according to the General acylation procedure 1, starting from 6-amino-1-methyl-1,3-dihydro-2H-benzo[d]imidazole-2-thione (**42**, 91 mg, 0.51 mmol), HATU (291 mg, 0.77 mmol), and 2-(pyridin-3-yl)acetic acid hydrochloride (134 mg, 0.77 mmol) to give compound **52** (85 mg, 56% yield) as a white solid. Mp.: 291 °C; ¹H NMR (500 MHz, DMSO-*d*₆) δ 12.69 (s, 1H), 10.87 (s, 1H), 8.94 (s, 1H), 8.84 (d, *J* = 5.4 Hz, 1H), 8.57 (d, *J* = 7.1 Hz, 1H), 8.03 (dd, *J* = 8.0, 5.7 Hz, 1H), 7.80 (d, *J* = 3.3 Hz, 1H), 7.33 (dd, *J* = 8.5, 1.8 Hz, 1H), 7.13 (d, *J* = 8.5 Hz, 1H), 4.06 (s, 2H), 3.57 (s, 3H); ¹³C NMR (126 MHz, DMSO-*d*₆) δ 168.52, 167.12, 146.60, 142.28, 140.18, 135.76, 134.35, 133.05, 126.81, 126.50, 114.76, 109.59, 100.48, 39.14, 29.85; HRMS (APCI⁺) *m/z* [M+H]⁺, calcd. for C₁₅H₁₅N₄O₂S: 299.0966, found: 299.0973; Purity by HPLC: 100%.

N-(3-methyl-2-thioxo-2,3-dihydro-1H-benzo[d]imidazole-5-yl)-3-(pyridin-3-yl)propanamide (55). The reaction was carried out according to the General acylation procedure 2, starting from 6-amino-1-methyl-1,3-dihydro-2H-benzo[d]imidazole-2-thione (**42**, 54 mg, 0.30 mmol), HATU (136 mg, 0.36 mmol), 3-(pyridin-3-yl)propanoic acid (54 mg, 0.36 mmol), and Et₃N (50 μL, 0.36 mmol) to give compound **55** (25 mg, 27% yield) as a white solid. Mp.: 128 °C; ¹H NMR (500 MHz, DMSO-*d*₆) δ 12.66 (s, 1H), 10.05 (s, 1H), 8.68–8.72 (m, 2H), 8.14 (d, *J* = 7.8 Hz, 1H), 7.72 (d, *J* = 12.2 Hz, 2H), 7.20 (dd, *J* = 8.5, 1.5 Hz, 1H), 7.10 (d, *J* = 8.5 Hz, 1H), 3.60 (s, 3H), 3.05 (t, *J* = 7.3 Hz, 2H), 2.74 (t, *J* = 7.3 Hz, 2H); ¹³C NMR (126 MHz, DMSO-*d*₆) δ 169.67, 168.54, 145.38, 143.35, 141.15, 134.42, 133.09, 126.59, 114.64, 109.57, 100.39, 36.65, 29.89, 27.62; HRMS (APCI⁺) *m/z* [M+H]⁺, calcd. for C₁₆H₁₇N₄O₂S: 313.1123, found: 313.1130. Purity by HPLC: 100%.

(R)-N-(3-methyl-2-thioxo-2,3-dihydro-1H-benzo[d]imidazole-5-yl)pyrrolidine-2-carboxamide (58). The reaction was carried out according to the General acylation procedure 1, starting from 6-amino-1-methyl-1,3-dihydro-2H-benzo[d]imidazole-2-thione (**42**, 95 mg, 0.53 mmol), HATU (242 mg, 0.64 mmol), and (R)-pyrrolidine-2-carboxylic acid (73 mg, 0.64 mmol) to give compound **58** (14 mg, 10% yield) as a white gum. ¹H NMR (500 MHz, DMSO-*d*₆) δ 10.14 (s, 1H), 7.77 (d, *J* = 1.6 Hz, 1H), 7.38 (dd, *J* = 8.5, 1.8 Hz, 1H), 7.12 (d, *J* = 8.5 Hz, 1H), 3.83 (dd, *J* = 8.6, 6.0 Hz, 1H), 3.61 (s, 3H), 2.98 (t, *J* = 6.8 Hz, 2H), 2.89 (s, 1H), 2.10 (dt, *J* = 18.2, 9.3 Hz, 1H), 1.84 (td, *J* = 13.0, 6.8 Hz, 1H), 1.72 (p, *J* = 6.8 Hz, 2H), resonance for NH missing; ¹³C NMR (126 MHz, DMSO-*d*₆) δ 171.83, 168.68, 133.78, 133.17, 126.86, 114.80, 109.52, 100.57, 60.56, 46.56, 38.22, 29.91, 25.38; HRMS (APCI⁺) *m/z* [M+H]⁺, calcd. for C₁₃H₁₇N₄O₂S: 277.1123, found: 277.1127; Purity by HPLC: 98%.

4.9. Preparation of 7-(acylamino)benzo[d]oxazole-2(3H)-thione derivatives 65, 67, and 69

N-(2-thioxo-2,3-dihydrobenzo[d]oxazol-7-yl)benzamide (65). The reaction was carried out according to the General acylation procedure 2, starting from 7-aminobenzo[d]oxazole-2(3H)-thione (**63**, 40 mg, 0.24 mmol), HATU (110 mg, 0.29 mmol), benzoic acid (35 mg, 0.29 mmol), and Et₃N (40 μL, 0.29 mmol) to give compound **65** (35 mg, 54% yield) as a white solid. Mp.: 218 °C; ¹H NMR (500 MHz, DMSO-*d*₆) δ 13.75 (s, 1H), 10.53 (s, 1H), 8.04–8.00 (m, 2H), 7.65–7.60 (m, 1H), 7.55 (dd, *J* = 10.3, 4.7 Hz, 2H), 7.36 (dd, *J* = 8.1, 0.8 Hz, 1H), 7.29 (t, *J* = 8.0 Hz, 1H), 7.10 (dd, *J* = 7.8, 0.9 Hz, 1H); ¹³C NMR (126 MHz, DMSO-*d*₆) δ 179.82, 165.22, 141.69, 133.62, 132.83, 131.94, 128.42, 127.85, 124.92, 121.38, 119.49, 107.41; HRMS (ESI⁺) *m/z* [M+H]⁺, calcd. for C₁₄H₁₁N₂O₂S: 271.0541, found: 271.0538; Purity by HPLC: 100%.

2-(Pyridin-3-yl)-N-(2-thioxo-2,3-dihydrobenzo[d]oxazol-7-

yl)acetamide (67). The reaction was carried out according to the General acylation procedure 2, starting from 7-aminobenzo[d]oxazole-2(3*H*)-thione (**63**, 40 mg, 0.24 mmol), HATU (110 mg, 0.29 mmol), 2-(pyridin-3-yl)acetic acid hydrochloride (50 mg, 0.29 mmol), and Et₃N (73 μ L, 0.53 mmol) to give compound **67** (35 mg, 51% yield) as a white solid. Mp.: 240 °C; ¹H NMR (500 MHz, DMSO-*d*₆) δ 13.93 (s, 1H), 10.55 (s, 1H), 8.57 (s, 1H), 8.49 (s, 1H), 7.78 (d, *J* = 7.8 Hz, 1H), 7.70 (d, *J* = 8.2 Hz, 1H), 7.39 (dd, *J* = 7.6, 4.8 Hz, 1H), 7.24 (t, *J* = 8.2 Hz, 1H), 7.00 (d, *J* = 7.8 Hz, 1H), 3.86 (s, 2H). ¹³C NMR (126 MHz, DMSO-*d*₆) δ 179.59, 169.05, 150.11, 147.73, 139.18, 136.80, 131.91, 131.41, 125.23, 123.38, 121.81, 116.75, 106.04, 39.02. HRMS (ESI⁺) *m/z* [M+H]⁺, calcd. for C₁₄H₁₂N₃O₂S: 286.0650, found: 286.0653; Purity by HPLC: 100%.

3-(Pyridin-3-yl)-*N*-(2-thioxo-2,3-dihydrobenzo[d]oxazol-7-yl)propanamide (69). The reaction was carried out according to the General acylation procedure 2, starting from 7-aminobenzo[d]oxazole-2(3*H*)-thione (**63**, 40 mg, 0.24 mmol), HATU (110 mg, 0.29 mmol), 3-(pyridin-3-yl)propanoic acid (44 mg, 0.29 mmol), and Et₃N (40 μ L, 0.29 mmol) to give compound **69** (24 mg, 33% yield) as a white solid. Mp.: 244–246 °C; ¹H NMR (500 MHz, DMSO-*d*₆) δ 13.93 (s, 1H), 10.24 (s, 1H), 8.55 (s, 1H), 8.46 (s, 1H), 7.76 (d, *J* = 7.7 Hz, 1H), 7.66 (d, *J* = 8.3 Hz, 1H), 7.38 (s, 1H), 7.24 (t, *J* = 8.1 Hz, 1H), 6.99 (d, *J* = 7.8 Hz, 1H), 2.97 (t, *J* = 7.5 Hz, 2H), 2.80 (t, *J* = 7.5 Hz, 2H). ¹³C NMR (126 MHz, DMSO-*d*₆) δ 179.56, 170.58, 149.17, 146.89, 140.86, 139.19, 136.31, 131.86, 125.21, 123.57, 121.87, 116.86, 105.89, 36.71, 27.82; HRMS (ESI⁺) *m/z* [M+H]⁺, calcd. for C₁₅H₁₄N₃O₂S: 300.0806, found: 300.0808; Purity by HPLC: 100%.

4.10. Preparation of 7-(acylamino)-1-methylbenzo[d]imidazole-2(3*H*)-thione derivatives 66, 68, and 70

***N*-(3-methyl-2-thioxo-2,3-dihydro-1*H*-benzo[d]imidazole-4-yl)benzamide (66).** The reaction was carried out according to the General acylation procedure 2, starting from 7-amino-1-methyl-1,3-dihydro-2*H*-benzo[d]imidazole-2-thione (**64**, 43 mg, 0.24 mmol), HATU (110 mg, 0.29 mmol), benzoic acid (35 mg, 0.29 mmol), and Et₃N (40 μ L, 0.29 mmol) to give compound **66** as a white solid (32 mg, 47% yield). Mp.: 295–298 °C; ¹H NMR (500 MHz, DMSO-*d*₆) δ 12.91 (s, 1H), 10.36 (s, 1H), 8.06–8.00 (m, 2H), 7.63 (t, *J* = 7.3 Hz, 1H), 7.56 (t, *J* = 7.5 Hz, 2H), 7.21 (t, *J* = 7.8 Hz, 1H), 7.16 (d, *J* = 7.8 Hz, 1H), 7.07 (d, *J* = 7.5 Hz, 1H), 3.74 (s, 3H); ¹³C NMR (126 MHz, DMSO-*d*₆) δ 169.20, 167.15, 133.72, 132.10, 131.95, 129.09, 128.60, 127.67, 122.86, 122.54, 121.24, 108.37, 31.29; HRMS (APCI⁺) *m/z* [M+H]⁺, calcd. for C₁₅H₁₄N₃O₂S: 180.0595, found: 180.0593; Purity by HPLC: 100%.

***N*-(3-methyl-2-thioxo-2,3-dihydro-1*H*-benzo[d]imidazole-4-yl)-2-(pyridin-3-yl)acetamide (68).** The reaction was carried out according to the General acylation procedure 2, starting from 7-amino-1-methyl-1,3-dihydro-2*H*-benzo[d]imidazole-2-thione (**64**, 43 mg, 0.24 mmol), HATU (110 mg, 0.29 mmol), 2-(pyridin-3-yl)acetic acid hydrochloride (50 mg, 0.29 mmol), and Et₃N (74 μ L, 0.53 mmol) to give compound **68** (16 mg, 22% yield) as a white solid. Mp.: 286 °C; ¹H NMR (500 MHz, DMSO-*d*₆) δ 12.85 (s, 1H), 10.10 (s, 1H), 8.58 (m, 2H), 7.82 (d, *J* = 7.7 Hz, 1H), 7.42 (s, 1H), 7.14 (t, *J* = 7.8 Hz, 1H), 7.09 (d, *J* = 7.7 Hz, 1H), 6.94 (d, *J* = 7.6 Hz, 1H), 3.79 (s, 2H), 3.60 (s, 3H); ¹³C NMR (126 MHz, DMSO-*d*₆) δ 170.35, 169.12, 149.85, 147.54, 137.25, 132.05, 128.64, 122.80, 122.08, 120.77, 108.22, 39.32, 31.25; HRMS (APCI⁺) *m/z* [M+H]⁺, calcd. for C₁₅H₁₅N₄O₂S: 299.0966, found: 299.0951; Purity by HPLC: 100%.

***N*-(3-methyl-2-thioxo-2,3-dihydro-1*H*-benzo[d]imidazole-4-yl)-3-(pyridin-3-yl)propanamide (70).** The reaction was carried out according to the General acylation procedure 2, starting from 7-amino-1-methyl-1,3-dihydro-2*H*-benzo[d]imidazole-2-thione (**64**, 43 mg, 0.24 mmol), HATU (110 mg, 0.29 mmol), 3-(pyridin-3-yl)propanoic acid (44 mg, 0.29 mmol), and Et₃N (40 μ L, 0.29 mmol) to

give compound **70** (32 mg, 43% yield) as a white solid. Mp.: 221 °C; ¹H NMR (500 MHz, DMSO-*d*₆) δ 12.84 (s, 1H), 9.87 (s, 1H), 8.87 (s, 1H), 8.80 (s, 1H), 8.52 (d, *J* = 8.0 Hz, 1H), 8.04–7.98 (m, 1H), 7.13 (t, *J* = 7.8 Hz, 1H), 7.08 (d, *J* = 7.4 Hz, 1H), 6.86 (d, *J* = 7.6 Hz, 1H), 3.60 (s, 3H), 3.14 (t, *J* = 7.2 Hz, 2H), 2.87 (t, *J* = 7.2 Hz, 2H); ¹³C NMR (126 MHz, DMSO-*d*₆) δ 171.59, 169.12, 145.55, 142.14, 140.29, 132.06, 128.63, 126.58, 122.81, 122.00, 120.76, 108.18, 35.26, 31.20, 27.25; HRMS (APCI⁺) *m/z* [M+H]⁺, calcd. for C₁₆H₁₇N₄O₂S: 313.1123, found: 313.1133; Purity by HPLC: 100%.

4.11. Procedure for the preparation of compound 59

To a solution of 3-bromo-2-fluoronitrobenzene (**VIII**, 1.10 g, 5.0 mmol, 1.0 equiv.) in 1,4-dioxane (40 mL), SnCl₂ × 2H₂O (5.64 g, 25.0 mmol, 5.0 equiv.) and two drops of 1 M HCl were added. The mixture was allowed to stir at room temperature for 2 h. Then, the volatiles were evaporated and the residue dissolved in EtOAc (80 mL). The organic phase was washed with 1 M NaOH (2 × 80 mL) and brine (40 mL), dried with MgSO₄, and evaporated. The product, 3-bromo-2-fluoroaniline (**IX**) was obtained as colorless oil (853 mg, 90% yield). Physical and spectroscopic data were identical to those reported previously [76].

To a solution of **IX** (760 mg, 4.0 mmol, 1.0 equiv.) in DMF (15 mL), potassium ethyl xanthogenate (1.41 g, 8.8 mmol, 2.2 equiv.) was added. The mixture was allowed to stir at 120 °C for 4 h. It was then cooled to room temperature, diluted with H₂O (60 mL), and the pH was adjusted to 1 with 10% HCl. The precipitate formed was filtered off and washed with H₂O (2 × 30 mL). The pure 7-bromobenzo[d]thiazole-2(3*H*)-thione (**59**) was obtained as a white solid (931 mg, 95% yield). ¹H NMR (400 MHz, DMSO-*d*₆) δ 14.05 (s, 1H), 7.52 (dd, *J* = 7.9, 1.0 Hz, 1H), 7.36 (t, *J* = 7.9 Hz, 1H), 7.30 (dd, *J* = 7.9, 1.0 Hz, 1H); HRMS (ESI⁺) *m/z* [M+H]⁺, calcd. for C₇H₅NS₂Br: 245.90413, found: 245.90388. Purity by HPLC: 95%.

4.12. General procedure for the preparation of 7-arylbenzo[d]thiazole-2(3*H*)-thione derivatives 61 and 62

In a screw cap vial, 7-bromobenzo[d]thiazole-2(3*H*)-thione (**59**, 1.0 equiv.) was dissolved in DMF (3 mL), followed by the addition of appropriate arylboronic acid (1.5 equiv.), K₂CO₃ (3.0 equiv.) and H₂O (0.3 mL). Nitrogen was bubbled through the mixture and then Pd(dppf)Cl₂ (0.1 equiv.) was added. The reaction was stirred at 140 °C for 16 h. The mixture was then cooled and the volatiles evaporated under reduced pressure. The crude product was partitioned between CH₂Cl₂ (10 mL) and H₂O (10 mL) and extracted. The organic phase was dried with Na₂SO₄, filtered, and evaporated. The products were purified by reversed phase flash column chromatography using CH₃CN:H₂O as an eluent system (gradient from 1:9 to 10:0).

7-Phenylbenzo[d]thiazole-2(3*H*)-thione (61). The reaction was carried out according to the General procedure, starting from 7-bromobenzo[d]thiazole-2(3*H*)-thione (**59**, 74 mg, 0.30 mmol), phenylboronic acid (55 mg, 0.45 mmol), K₂CO₃ (124 mg, 0.90 mmol), and Pd(dppf)Cl₂ (22 mg, 0.03 mmol) to give 7-phenylbenzo[d]thiazole-2(3*H*)-thione (**61**, 14 mg, 19% yield) as a brown solid. Mp.: 139–143 °C; ¹H NMR (500 MHz, DMSO-*d*₆) δ 13.88 (s, 1H), 7.60 (d, *J* = 7.3 Hz, 2H), 7.56–7.50 (m, 3H), 7.46 (t, *J* = 7.3 Hz, 1H), 7.39 (d, *J* = 7.5 Hz, 1H), 7.33 (d, *J* = 8.0 Hz, 1H); ¹³C NMR (126 MHz, DMSO-*d*₆) δ 189.15, 141.93, 138.21, 134.67, 129.20, 128.56, 127.99, 127.66, 127.33, 123.78, 111.57; HRMS (APCI⁺) *m/z* [M+H]⁺, calcd. for C₁₃H₁₀NS₂: 244.0254, found: 244.0244; Purity by HPLC: 99%.

3-(2-Thioxo-2,3-dihydrobenzo[d]thiazol-7-yl)benzonitrile (62). The reaction was carried out according to the General procedure, starting from 7-bromobenzo[d]thiazole-2(3*H*)-thione (**59**,

74 mg, 0.30 mmol), (3-cyanophenyl) boronic acid (66 mg, 0.45 mmol), K_2CO_3 (124 mg, 0.90 mmol), and $Pd(dppf)Cl_2$ (22 mg, 0.03 mmol) to give 3-(2-thioxo-2,3-dihydrobenzo[d]thiazol-7-yl) benzonitrile (**62**, 10 mg, 12% yield) as a brown solid. Mp.: 161 °C; 1H NMR (500 MHz, $DMSO-d_6$) δ 13.92 (s, 1H), 8.05 (s, 1H), 7.92 (t, $J = 7.4$ Hz, 2H), 7.73 (t, $J = 7.8$ Hz, 1H), 7.53 (t, $J = 7.8$ Hz, 1H), 7.44 (d, $J = 7.1$ Hz, 1H), 7.35 (d, $J = 7.8$ Hz, 1H); ^{13}C NMR (126 MHz, $DMSO-d_6$) δ 188.90, 142.02, 139.30, 132.53, 132.18, 132.05, 131.05, 130.39, 128.05, 127.80, 124.12, 118.30, 112.37, 112.31; HRMS (APCI⁺) m/z $[M+H]^+$, calcd. for $C_{14}H_9N_2S_2$: 269.0207, found: 269.0200; Purity by HPLC: 100%.

4.13. Procedure for the synthesis of *N*-(benzo[d]thiazol-2-yl) acrylamide [79]

A round bottom flask was charged with 2-aminobenzothiazole (300 mg, 2.0 mmol) and dry THF (15 mL) under argon atmosphere, and cooled on an ice bath (0 °C). Et_3N (0.56 mL, 4.0 mmol, 2.0 equiv.) and acryloyl chloride (0.24 mL, 3.0 mmol, 1.5 equiv.) were added subsequently at 0 °C. The mixture was stirred for 30 min at 0 °C and then overnight at room temperature. The solvent was then evaporated and the residue was dissolved in CH_2Cl_2 (50 mL) and washed with H_2O (30 mL). The organic phase was dried with Na_2SO_4 , filtered, and the solvent evaporated to give the crude product. The pure compound was obtained by first performing flash column chromatography using $EtOAc:n$ -hexane (1:1) as an eluent system, followed by recrystallization from $EtOAc$ to give **79** (60 mg, 15% yield) as a white solid. Mp.: 187–189 °C; 1H NMR (400 MHz, $DMSO-d_6$) δ 12.61 (s, 1H), 8.10–7.90 (m, 1H), 7.76 (d, $J = 8.0$ Hz, 1H), 7.45 (ddd, $J = 8.2, 7.1, 1.3$ Hz, 1H), 7.32 (ddd, $J = 8.0, 7.4, 1.1$ Hz, 1H), 6.58 (dd, $J = 17.1, 10.0$ Hz, 1H), 6.46 (dd, $J = 17.1, 1.8$ Hz, 1H), 5.97 (dd, $J = 10.0, 1.8$ Hz, 1H). ^{13}C NMR (101 MHz, $DMSO-d_6$) δ 163.64, 157.91, 148.62, 131.65, 130.17, 129.41, 126.17, 123.67, 121.76, 120.62; HRMS (ESI⁺) m/z $[M+H]^+$, calcd. for $C_{10}H_9N_2OS$: 205.0430, found: 205.0429. Purity by HPLC: 95%.

4.14. Procedure for the synthesis of *N*-(1-methyl-1*H*-benzo[d]imidazole-2-yl)acrylamide [80]

A round bottom flask was charged with 2-amino-1-methylbenzimidazole (300 mg, 2.04 mmol) and dry THF (10 mL) under argon atmosphere, and cooled on an ice bath (0 °C). Et_3N (0.57 mL, 4.08 mmol, 2.0 equiv.) and acryloyl chloride (0.25 mL, 3.06 mmol, 1.5 equiv.) were added subsequently at 0 °C. The mixture was stirred for 30 min at 0 °C and then overnight at room temperature. The solvent was then evaporated and the residue was dissolved in CH_2Cl_2 (50 mL) and washed with H_2O (30 mL). The organic phase was dried with Na_2SO_4 , filtered, and the solvent evaporated to give crude product, which was purified by flash column chromatography using $EtOAc:n$ -hexane (1:1) as an eluent system to give **80** (55 mg, 13% yield) as a white solid. Mp.: 134–136 °C; 1H NMR (400 MHz, $CDCl_3$) δ 12.33 (s, 1H), 7.34–7.20 (m, 4H), 6.52–6.38 (m, 2H), 5.70 (t, $J = 6.1$ Hz, 1H), 3.69 (s, 3H); ^{13}C NMR (101 MHz, $CDCl_3$) δ 176.44, 153.85, 137.09, 130.27, 128.50, 126.25, 123.20, 123.16, 111.47, 109.10, 28.36; HRMS (ESI⁺) m/z $[M+H]^+$, calcd. for $C_{11}H_{12}N_3O$: 202.0975, found: 202.0975; Purity by HPLC: 98%.

4.15. Preparation of 2-amino-6-chlorobenzenethiol (XXI)

To a solution of 2,3-dichloroaniline (XIV, 2.37 mL, 20.0 mmol, 1.0 equiv.) in DMF (16 mL), potassium ethyl xanthogenate (3.85 g, 24.0 mmol, 1.2 equiv.) was added and the mixture stirred at 140 °C for 3 h. It was then cooled to room temperature, diluted with H_2O (60 mL) and the pH was adjusted to 1 with 10% HCl. The precipitate

formed was filtered off and washed with H_2O (2×30 mL). The pure compound 7-chlorobenzo[d]thiazole-2(3*H*)-thione (**12**) was obtained as a white solid (3.24 mg, 80% yield). Physical and spectroscopic data were identical to those reported previously [77].

Compound **12** (807 mg, 4.0 mmol) was dissolved in hydrazine hydrate (20 mL) and the mixture stirred at 110 °C for 16 h. After the reaction was complete, the mixture was diluted with H_2O (30 mL) and the pH was adjusted to 7 with 10% HCl. The aqueous phase was extracted with $EtOAc$ (2×50 mL) and the organic layer subsequently washed with brine (20 mL), dried with $MgSO_4$, and evaporated. The product, 2-amino-6-chlorobenzenethiol (**XXI**), was purified by reversed phase flash column chromatography using eluents A (0.1% HCOOH in MeCN) and B (0.1% HCOOH in H_2O) (gradient from 1:9 to 10:0). Yellow solid (194 mg, 30% yield). According to LC-MS, the product contained desired thiol compound **XXI**, but also the *in situ* formed disulfide in a substantial amount (38%); therefore, it was transferred to the next reaction step immediately.

4.16. Preparation of 5-chloro-*N*¹-methylbenzene-1,2-diamine (XXIV)

To a cooled (0 °C) solution of 5-chloro-2-nitroaniline (**XV**, 690 mg, 4.0 mmol, 1.0 equiv.) in THF (10 mL), NaH (60% suspension in paraffin oil, 352 mg, 8.8 mmol, 2.2 equiv.) was slowly added, and the mixture was allowed to stir for 15 min. Then, MeI (374 μ L, 6.0 mmol, 1.5 equiv.) was added dropwise and the mixture stirred at room temperature for 2 h. After the reaction was complete, $EtOAc$ (50 mL) was added and the organic phases washed with H_2O (30 mL), brine NaCl (20 mL), dried with $MgSO_4$, and evaporated under reduced pressure. The product, 5-chloro-*N*-methyl-2-nitroaniline (**XVII**, 707 mg, 95% yield) was obtained as a yellow solid. Physical and spectroscopic data were identical to those reported previously [78].

Compound **XVII** (601 mg, 3.22 mmol, 1.0 equiv.) was dissolved in $EtOAc$ (50 mL), followed by the addition of $SnCl_2 \times 2H_2O$ (5.81 g, 25.76 mmol, 8.0 equiv.). The mixture was stirred at reflux for 16 h. Then, it was diluted with $EtOAc$ (150 mL), washed with saturated aqueous solution of $NaHCO_3$ (2×150 mL), brine NaCl (50 mL), dried with $MgSO_4$, and evaporated under reduced pressure. The product, 5-chloro-*N*¹-methylbenzene-1,2-diamine (**XXIV**, 443 mg, 88%) was obtained as a yellow oil. Physical and spectroscopic data were identical to those reported previously [78].

4.17. Preparation of 6-chloro-*N*¹-methylbenzene-1,2-diamine (XXV)

To a cooled (0 °C) solution of 2-chloro-6-nitroaniline (**XVI**, 690 mg, 4.0 mmol, 1.0 equiv.) in THF (10 mL) in a screw cap vial, NaH (60% suspension in paraffin oil, 352 mg, 8.8 mmol, 2.2 equiv.) was added portionwise and the mixture was allowed to stir for 15 min. Then, MeI (374 μ L, 6.0 mmol, 1.5 equiv.) was added dropwise and the mixture stirred at 50 °C overnight. After the reaction was complete, $EtOAc$ (50 mL) was added and the organic phases washed with H_2O (30 mL), brine NaCl (20 mL), dried with $MgSO_4$, and evaporated under reduced pressure. The product, 2-chloro-*N*-methyl-6-nitroaniline (**XVIII**), was purified by reversed phase flash column chromatography using eluents A (0.1% HCOOH in MeCN) and B (0.1% HCOOH in H_2O) (gradient from 1:9 to 10:0). Red solid (326 mg, 44% yield). Mp.: 45 °C; 1H NMR (500 MHz, $DMSO-d_6$) δ 7.73 (dd, $J = 8.3, 1.5$ Hz, 1H), 7.60 (dd, $J = 7.8, 1.5$ Hz, 1H), 6.75 (t, $J = 8.1$ Hz, 1H), 6.61 (d, $J = 4.7$ Hz, 1H), 2.75 (d, $J = 5.3$ Hz, 3H); ^{13}C NMR (126 MHz, $DMSO-d_6$) δ 141.21, 136.79, 134.02, 125.18, 122.12, 116.13, 32.74; HRMS (APCI⁺) m/z $[M+H]^+$, calcd. for $C_7H_8ClN_2O_2$: 187.0274 and 189.0245, found: 187.0262 and 189.0232; Purity by HPLC: 99%.

Compound **XVIII** (250 mg, 1.34 mmol, 1.0 equiv.) was dissolved in EtOAc (30 mL), followed by the addition of $\text{SnCl}_2 \times \text{H}_2\text{O}$ (2.42 g, 10.72 mmol, 8.0 equiv.) The mixture was stirred at reflux for 16 h. Then, it was diluted with EtOAc (100 mL), washed with saturated aqueous solution of NaHCO_3 (2×100 mL), brine NaCl (50 mL), dried with MgSO_4 , and evaporated under reduced pressure. The product, 6-chloro-*N*¹-methylbenzene-1,2-diamine (**XXV**) was purified by reversed phase flash column chromatography using A (0.1% HCOOH in MeCN) and B (0.1% HCOOH in H_2O) (gradient from 1:9 to 10:0). Brown oil (53 mg, 25% yield). Despite purification, impurities were present and this product was used in the next reaction step.

4.18. General procedure for the preparation of chloro-substituted benzoXazole-2-carbonitriles **84**, **85**, and **88-92**

To a solution of an appropriate chloro-substituted aniline derivative (1.0 equiv.) in pyridine (6 mL for 1.0 mmol of aniline), Appel's salt (1.0 or 1.2 equiv.) was added portionwise. The reaction mixtures were stirred at different temperatures and the reaction time was varied as well (see below). After the reaction was complete, the volatiles were removed under reduced pressure and the crude residue was purified by reversed phase flash column chromatography using eluents A (0.1% HCOOH in MeCN) and B (0.1% HCOOH in H_2O) (gradient from 1:9 to 10:0).

6-Chloro-1,3-benzoxazole-2-carbonitrile (84). The reaction was carried out according to the General procedure by using 2-amino-5-chlorophenol (**XIX**, 144 mg, 1.0 mmol, 1.0 equiv.) and Appel's salt (250 mg, 1.2 mmol, 1.2 equiv.). The mixture was initially stirred at room temperature for 3 h and then heated to reflux for 16 h. After purification, the product **84** (43 mg, 24% yield) was obtained as a brown solid. Mp.: 90 °C; ^1H NMR (500 MHz, $\text{DMSO}-d_6$) δ 8.19 (d, $J = 1.9$ Hz, 1H), 8.04–7.99 (m, 1H), 7.65 (dd, $J = 8.6, 1.9$ Hz, 1H). ^{13}C NMR (126 MHz, $\text{DMSO}-d_6$) δ 150.18, 137.92, 137.87, 133.79, 127.32, 122.61, 112.52, 109.47. Purity by HPLC: 98%; HRMS measurements (ESI, APCI) were done, but the compound was not ionizable. To further confirm the structure, we performed 2D NMR experiments (see Supporting Information, Figures S14 and S15).

7-Chloro-1,3-benzoxazole-2-carbonitrile (85). The reaction was carried out according to the General procedure by using 2-amino-6-chlorophenol (**XX**, 144 mg, 1.0 mmol, 1.0 equiv.) and Appel's salt (250 mg, 1.2 mmol, 1.2 equiv.). The mixture was initially stirred at room temperature for 3 h and then heated to reflux for 16 h. After purification, the product **85** (30 mg, 17% yield) was obtained as a brown solid. Mp.: 87 °C; ^1H NMR (500 MHz, $\text{DMSO}-d_6$) δ 7.97 (d, $J = 8.1$ Hz, 1H), 7.82 (d, $J = 8.0$ Hz, 1H), 7.60 (t, $J = 8.1$ Hz, 1H); ^{13}C NMR (126 MHz, $\text{DMSO}-d_6$) δ 146.32, 140.15, 137.64, 129.04, 127.72, 120.58, 115.36, 109.30; Purity by HPLC: 98%. HRMS measurements (ESI, APCI) were done, but the compound was not ionizable. To further confirm the structure, we performed 2D NMR experiments (see Supporting Information Figures S16 and S17).

7-Chloro-1,3-benzothiazole-2-carbonitrile (88). The reaction was carried out according to the General procedure by using 2-amino-6-chlorobenzenethiol (**XXI**, starting material contained the *in situ* formed disulfide, 148 mg) and Appel's salt (194 mg, 0.93 mmol). The mixture was stirred at room temperature for 16 h. After purification, the product **88** (54 mg, 30% yield) was obtained as a brown solid. Mp. 89 °C; ^1H NMR (500 MHz, $\text{DMSO}-d_6$) δ 8.25 (d, $J = 8.3$ Hz, 1H), 7.85 (d, $J = 7.7$ Hz, 1H), 7.75 (t, $J = 8.1$ Hz, 1H); ^{13}C NMR (126 MHz, $\text{DMSO}-d_6$) δ 151.97, 137.44, 135.35, 129.57, 128.25, 125.80, 123.63, 112.78; HRMS (APCI⁺) m/z $[\text{M}+\text{H}]^+$, calcd. for $\text{C}_8\text{H}_4\text{ClN}_2\text{S}$: 194.9783 and 196.9754, found: 194.9777 and 196.9740; Purity by HPLC: 99%.

6-Chloro-1H-benzimidazole-2-carbonitrile (89). The reaction was carried out according to the General procedure by using 4-

chlorobenzene-1,2-diamine (**XXII**, 143 mg, 1.0 mmol, 1.0 equiv.) and Appel's salt (209 mg, 1.0 mmol, 1.0 equiv.). The mixture was initially stirred at room temperature for 2 h and then heated to reflux for 2 h. After purification, the product **89** (100 mg, 56% yield) was obtained as a light brown solid. Mp.: 195 °C; ^1H NMR (500 MHz, $\text{DMSO}-d_6$) δ 13.92 (br s, 1H), 7.81 (s, 1H), 7.74 (d, $J = 8.8$ Hz, 1H), 7.41 (dd, $J = 8.8, 1.9$ Hz, 1H); ^{13}C NMR (126 MHz, $\text{DMSO}-d_6 + \text{TFA}-d$) δ 138.83, 136.90, 129.95, 125.66, 118.19, 116.38, 114.15, 112.40; HRMS (APCI⁺) m/z $[\text{M}+\text{H}]^+$, calcd. for $\text{C}_8\text{H}_5\text{ClN}_3$: 178.0172 and 180.0142, found: 178.0165 and 180.0138; Purity by HPLC: 100%.

7-Chloro-1H-benzimidazole-2-carbonitrile (90). The reaction was carried out according to the General procedure by using 3-chlorobenzene-1,2-diamine (**XXIII**, 143 mg, 1.0 mmol, 1.0 equiv.) and Appel's salt (209 mg, 1.0 mmol, 1.0 equiv.). The mixture was initially stirred at room temperature for 2 h and then heated to reflux for 2 h. After purification, the product **90** (103 mg, 56% yield) was obtained as a light brown solid. Mp.: 175–180 °C; ^1H NMR (500 MHz, $\text{DMSO}-d_6$) δ 14.42 (br s, 1H), 7.67 (d, $J = 8.2$ Hz, 1H), 7.48 (d, $J = 7.6$ Hz, 1H), 7.41 (t, $J = 7.9$ Hz, 1H); ^{13}C NMR (126 MHz, $\text{DMSO}-d_6 + \text{TFA}-d$) δ 137.84, 126.48, 125.63, 124.55, 122.63, 114.59, 114.39, 112.54; HRMS (APCI⁺) m/z $[\text{M}+\text{H}]^+$, calcd. for $\text{C}_8\text{H}_5\text{ClN}_3$: 178.0172 and 180.0142, found: 178.0169 and 180.0138; Purity by HPLC: 98%.

6-Chloro-1-methyl-1H-benzimidazole-2-carbonitrile (91). The reaction was carried out according to the General procedure by using 5-chloro-*N*¹-methylbenzene-1,2-diamine (**XXIV**, 222 mg, 1.42 mmol, 1.0 equiv.) and Appel's salt (296 mg, 1.42 mmol, 1.0 equiv.) The mixture was initially stirred at room temperature for 2 h and then heated to reflux for 2 h. After purification, the product **91** (145 mg, 53% yield) was obtained as a light brown solid. Mp.: 140–145 °C; ^1H NMR (500 MHz, $\text{DMSO}-d_6$) δ 7.96 (d, $J = 1.9$ Hz, 1H), 7.81–7.78 (m, 1H), 7.43–7.38 (m, 1H), 3.97 (s, 3H); ^{13}C NMR (126 MHz, $\text{DMSO}-d_6$) δ 140.38, 135.37, 130.70, 127.85, 124.59, 121.97, 111.75, 111.17, 31.59; HRMS (APCI⁺) m/z $[\text{M}+\text{H}]^+$, calcd. for $\text{C}_9\text{H}_7\text{ClN}_3$: 192.0328 and 194.0299, found: 192.0318 and 194.0287; Purity by HPLC: 98%.

7-Chloro-1-methyl-1H-benzimidazole-2-carbonitrile (92). The reaction was carried out according to the General procedure by using 6-chloro-*N*¹-methylbenzene-1,2-diamine (**XXV**, 32 mg, 0.20 mmol, 1.0 equiv.) and Appel's salt (43 mg, 0.20 mmol, 1.0 equiv.) The mixture was initially stirred at room temperature for 2 h and then heated to reflux for 1 h. After purification, the product **92** (10 mg, 26% yield) was obtained as a brown solid. Mp.: 75–77 °C; ^1H NMR (500 MHz, $\text{DMSO}-d_6$) δ 7.79 (d, $J = 8.3$ Hz, 1H), 7.55 (d, $J = 7.7$ Hz, 1H), 7.39 (t, $J = 8.0$ Hz, 1H), 4.22 (s, 3H); ^{13}C NMR (126 MHz, $\text{DMSO}-d_6$) δ 143.83, 130.56, 128.95, 127.01, 124.92, 120.15, 116.48, 111.08, 34.33; HRMS (APCI⁺) m/z $[\text{M}+\text{H}]^+$, calcd. for $\text{C}_9\text{H}_7\text{ClN}_3$: 192.0328 and 194.0299, found: 192.0329 and 194.0297; Purity by HPLC: 99%.

4.19. Residual activity measurements

The preliminary screening of compounds was performed at 10 μM or 100 μM final concentrations in the assay buffer (0.01% SDS, 50 mM Tris-HCl, 0.5 mM EDTA, pH 7.4. To 50 μL of each compound, 25 μL 0.8 nM human iCP (Boston Biochem, Inc., Cambridge, MA, USA) was added. After 30 min incubation at 37 °C, the reaction was initiated by the addition of 25 μL 100 μM succinyl-Leu-Leu-Val-Tyr-7-amino-4-methylcoumarin (Suc-LLVY-AMC) (Bachem, Bubendorf, Switzerland) (final concentration was 25 μM). The reaction progress was recorded on the BioTek Synergy HT microplate reader by monitoring fluorescence at 460 nm ($\lambda_{\text{ex}} = 360$ nm) for 90 min at 37 °C. The initial linear ranges were used to calculate the velocity and to determine the residual activity. To determine the residual

activity of selected compounds in the reducing environment, TCEP (final concentration of 1 mM) was added to the assay buffer. In specific cases, (Suc-LLVY)₂R110 (AAT Bioquest, Sunnyvale, CA, USA) was used as a substrate to evaluate compounds for inhibition of β 5i and β 5 activities. Here, the fluorescence was monitored at 525 nm ($\lambda_{\text{ex}} = 495$ nm).

In the case of evaluation of β 1, β i, β 2, β 2i, and β 5 activities (note: the same concentration of human cCP was used [Boston Biochem, Inc., Cambridge, MA, USA]), the assay buffer was modified by adding the proteasomal activator PA28 α (Boston Biochem, Inc., Cambridge, MA, USA). After 30 min of incubation at 37 °C, the reaction was initiated by the addition of the relevant fluorogenic substrate: acetyl-Nle-Pro-Nle-Asp-AMC (Ac-nLPnLD-AMC, [Bachem, Bubendorf, Switzerland]) for β 1, acetyl-Pro-Ala-Leu-7-amino-4-methylcoumarin (Ac-PAL-AMC [Boston Biochem, Inc., Cambridge, MA, USA]) for β 1i, *t*-butyloxycarbonyl-Leu-Arg-7-amino-4-methylcoumarin (Boc-LRR-AMC, [Bachem, Bubendorf, Switzerland]) for β 2 and β 2i, Suc-LLVY-AMC for β 5. The fluorescence was monitored at 460 nm ($\lambda_{\text{ex}} = 360$ nm) for 90 min at 37 °C.

4.20. Determination of IC₅₀ values

The final assay mixtures contained 0.2 nM human iCP or 0.2 nM human cCP in the assay buffer (0.01% SDS, 50 mM Tris-HCl, 0.5 mM EDTA, pH 7.4). Inhibitors were dissolved in DMSO and added to black 96-well plates for at least eight different concentrations (the final concentration of DMSO did not exceed 1%). After 30 min of incubation at 37 °C, the reaction was initiated by the addition of the relevant fluorogenic substrate: Suc-LLVY-AMC for β 5i and β 5. The fluorescence was monitored at 460 nm ($\lambda_{\text{ex}} = 360$ nm) for 90 min at 37 °C. The progress of the reactions was recorded and the initial linear ranges were used to calculate the velocity. IC₅₀ values were calculated using GraphPadPrism (GraphPad Software, San Diego, CA, USA) and are means from at least three independent determinations. In specific cases, (Suc-LLVY)₂R110 (Sunnyvale, CA, USA) was used as a substrate to determine IC₅₀ values for inhibition of β 5i and β 5 activities. Here, the fluorescence was monitored at 525 nm ($\lambda_{\text{ex}} = 495$ nm).

To determine the IC₅₀ shift for selected compounds on the β 5i subunit, the same protocol was used, except for the 0 min of incubation timer prior to the addition of the substrate Suc-LLVY-AMC.

4.21. Reactivity assays

4.21.1. Horseradish peroxidase-phenol (HRP-PR) red assay

This assay was performed using a modified procedure described previously [64]. The HRP-PR detection reagent contained phenol red (300 μ g/mL) and HRP (180 μ g/mL) in buffer (50 mM HEPES, 50 mM NaCl, pH 7.5). Compounds were prepared as 10 mM DMSO stock solutions. DTT solution (3 mM) in buffer was freshly prepared every day to avoid oxidation. The reaction was performed in a 96-well microplate. To each well, 66 μ L of buffer, 2 μ L of 10 mM compound stock solution and 66 μ L of buffer (redox-free) or 66 μ L of 3 mM DTT solution was added. The resulting solution was incubated for 15 min at room temperature and absorbance at 610 nm was checked for assay interference. Next, 66 μ L of HRP-PR detection reagent was added and incubated for 5 min at room temperature. Finally, the reaction was terminated with the addition of 10 μ L of NaOH solution (1 M), and absorbance was measured at 610 nm using a 96-well microplate reader (Synergy H4, BioTek Instruments, Inc., Winooski, VT, USA). Final concentrations were: 100 μ M compound, 100 μ g/mL (282 μ M) phenol red, 60 μ g/mL HRP, 1 mM DTT, 1% DMSO. Duplicates were used for every compound in both redox-free and DTT conditions. To determine the blank value, compound solution was replaced with pure DMSO. Measured

absorbance for each compound was then divided by blank value. Threshold for activity flag was greater than 10-fold the standard deviation over DMSO blanks. 3-Methyltoxoflavin and NSC-663284 (6-chloro-7-(2-morpholin-4-yl-ethylamino)quinoline-5,8-dione) were used as positive controls.

4.21.2. H₂DCFDA assay

This assay was performed using a newly developed procedure. 2',7'-Dichlorodihydrofluorescein diacetate (H₂DCFDA) was prepared as 5 mM stock in DMSO and diluted 10-fold to 500 μ M with NaOH (0.01 M). Probe was freshly prepared for every plate and kept in the dark at room temperature for 30 min to hydrolyze the ester. Compounds were prepared as 10 mM DMSO stock solutions. The reactions were carried out in a black 96-well microplate at final volume of 150 μ L of buffer (50 mM HEPES, 50 mM NaCl, pH 7.5), containing 100 μ M compound, 50 μ M H₂DCFDA, 100 μ M TCEP and 1% of DMSO. Duplicates were used for every compound and in a parallel redox-free experiment, TCEP was omitted. The microplate was covered with a lid and kept in dark at room temperature for 30 min. The fluorescence intensity was then measured with 485 nm excitation and 535 nm emission filters (Synergy H4, BioTek Instruments, Inc., USA). To determine the blank value, compound solution was replaced with pure DMSO. Measured fluorescence for each compound was then divided by blank value. Threshold for activity flag was greater than 10-fold the standard deviation over DMSO blanks. 5-Aminoquinolin-8-ol was used as a positive control.

4.21.3. Resazurin assay

Resazurin stock solution (10 mM) and DTT stock solution (3 mM) in buffer (50 mM HEPES, 50 mM NaCl, pH 7.5) were freshly prepared every day. The reactions were carried out in a black 96-well microplate at final volume of 200 μ L of buffer, containing 0.1, 1.0, or 10 μ M of compound, 5 μ M resazurin, 100 μ M DTT and 1% of DMSO. Duplicates were used for every compound concentration. The microplate was covered with a lid and kept in dark at room temperature for 30 min. The fluorescence intensity was then measured with 560 nm excitation and 590 nm emission filters (Synergy H4, BioTek Instruments, Inc., USA). To determine the blank value, compound solution was replaced with pure DMSO. The fluorescence, measured for each compound, was then divided by blank value. Threshold for activity flag was greater than 10-fold the standard deviation over DMSO blanks. Menadione was used as a positive control.

4.21.4. NMR assay

NMR spectra were recorded on a Bruker Avance III 400 MHz spectrometer at 295 K. Compound stock solution (40 mM) was prepared in DMSO-*d*₆ and diluted to 4 mM (10% DMSO-*d*₆) with potassium phosphate buffer (100 mM, pH 7.4, 20% D₂O). 500 μ L of this solution was added to an NMR tube and a spectrum at 0 h was recorded. GSH (20 mM) was dissolved in potassium phosphate buffer with 10% DMSO-*d*₆ and 500 μ L was added to the NMR tube with compound solution. The final concentrations were: 2 mM compound, 10 mM GSH, 10% DMSO-*d*₆ in 100 mM potassium phosphate buffer. The reaction was monitored at room temperature with NMR for 19 h at multiple time points. Benzoisothiazolone was used as a positive control.

4.21.5. HPLC-MS assay

This assay was performed using a modified procedure described previously [81]. Briefly, compound stock solution (10 mM) was prepared in MeCN and GSH stock solution (10 mM) in PBS buffer. Then, compound stock solution was 20-fold diluted with PBS buffer and MeCN concentration was adjusted to 10%. 250 μ L of the resulting solution was mixed with 250 μ L of GSH stock solution and

incubated at 37 °C overnight. The final concentrations were: 0.25 mM compound, 5 mM GSH and 5% MeCN in PBS buffer at four different pH values (7.4, 8.0, 8.5, and 9.0). Before injection, sample solution was diluted 5-fold with MeCN/H₂O = 4/1, V/V. HPLC-MS measurements were performed using a Shimadzu LCMS-2020 device equipped with Reprospher 100 C18 Column (3.0 × 100 mm; 5 μm). Flow rate was set to 1 mL/min, column temperature was kept at 40 °C and 4 μL of sample solution was injected. An eluent system of A (H₂O/MeCN/HCOOH = 95/5/1) and B (H₂O/MeCN/HCOOH = 5/95/1) was used with gradient elution: 0–2 min, 0% A → 100% A; 2–2.5 min, 100% A; 2.5–3 min, 100% A → 0% A; 3–4 min, 0% A. Adducts were detected using photodiode array detector (190–800 nm) and quadrupole positive-negative double ion MS analyser in a range of 50–1000 *m/z*.

4.21.6. High-throughput thiol reactivity assay

The assay was performed using a modified procedure described previously [67]. Briefly, DTNB stock solution (2.5 mM) and TCEP stock solution (20 mM) were freshly prepared before performing experiments. The reaction was performed at 37 °C in a 96-well microplate with a final volume of 300 μL of buffer (20 mM sodium phosphate buffer, 150 mM NaCl, pH 7.4), containing 100 μM compound, 100 μM TCEP, 25 μM DTNB (giving 50 μM TNB²⁻) and 5% DMSO. The plate was covered with a lid, incubated at 37 °C inside the plate reader and after 15 min incubation the absorbance at 412 nm was measured (Synergy H4, BioTek Instruments, Inc., USA). Absorbances were acquired every 5 min for up to 24 h using Gen5 software (BioTek Instruments, Inc., USA). Duplicates were used for each compound and a parallel experiment without DTNB was performed to determine the compound background absorbance. Next, compound background absorbance was subtracted from each measurement. Reactivity was determined after 4 h with threshold greater than 3-fold the standard deviation over the DMSO blanks. Compounds were labelled as highly reactive if the plateau was reached in the first 10 h. 2-Chloro-*N*-(3-chlorophenyl)acetamide was used as a positive control.

4.21.7. TNB²⁻ depletion assays

4.21.7.1. High-throughput absorbance. TNB²⁻ stock solution (10 mM) was freshly prepared every day. The reaction was performed in a 96-well microplate at final volume of 300 μL of buffer (20 mM sodium phosphate buffer, 150 mM NaCl, pH 7.4), containing 200 μM compound, 100 μM TNB²⁻ and 5% of DMSO. The plate was covered with a lid and absorbance was immediately measured at 412 nm (Synergy H4, BioTek Instruments, Inc., USA). The plate was incubated at 37 °C inside the plate reader and the absorbances were acquired every 5 min for 12–24 h. After completion of the reaction, 5 μL of TCEP was added at a final concentration of 200 μM. The absorbance was measured again at 412 nm after 2 h of incubation at 37 °C. Duplicates were used for every compound and a parallel experiment without TNB²⁻ was performed to determine compound background absorbance. Baseline was determined from an experiment, where compound solution was replaced with pure DMSO. Compound background absorbance and baseline were subtracted from each measurement using Gen5 software (BioTek Instruments, Inc., USA). Reactivity was determined after 12 h with threshold greater than 3-fold the standard deviation over the DMSO blanks. 2-Chloro-*N*-(3-chlorophenyl)acetamide was used as a positive control.

4.21.7.2. NMR. Compound **29** (6 mM) was incubated with TNB²⁻ (3 mM) in buffer (20 mM sodium phosphate buffer, 150 mM NaCl, pH 7.4, 20% D₂O). The content of DMSO was 5%. NMR spectrum was immediately acquired on a Bruker Avance III 400 MHz spectrometer with standard parameter set WATERSUP (noesygppr1d). The

reaction was then followed for 24 h. For a blank experiment, only TNB²⁻ was added to the buffer (Figure S10).

4.20.7.3. HRMS. Compound (200 μM) was incubated with TNB²⁻ (100 μM) in a volatile buffer (20 mM ammonium formate, pH 7.4) for 30 min at room temperature. The final content of DMSO was 5%. Sample solution was 40-fold diluted with H₂O/MeOH = 3/2, V/V, and directly injected. Mass spectra were recorded using a Thermo Scientific Q Exactive Plus mass spectrometer in full scan and SIM mode. Peaks within 5 ppm of calculated mass were examined. In a separate experiment, TNB²⁻ was substituted with GSH.

4.22. Microscale thermophoresis

Microscale thermophoresis measurements were conducted on a NanoTemper Monolith NT.115 device (Nanotemper, München, Germany), as detailed in our earlier work [44]. Briefly, human proteasome β5i subunit (cat. no: ENZ-670, ProSpec-Tany TechnoGene Ltd., Rehovot, Israel) was labelled with RED fluorescent NT-647-NHS dye (Nanotemper, cat. no: L001), after transferring from the vendor buffer to 20 mM phosphate buffer (pH 8.0) with 10% glycerol. Ligands were dissolved in DMSO and diluted into the protein buffer, with final DMSO concentrations not exceeding 1%. Single-point binding measurements at 100 μM ligand concentration (with 0.44 μM protein, 20% LED power) revealed fluorescence changes significantly different from the DMSO control for the assayed compounds and the known inhibitors PR-957 and compound **42**. Titration curves were acquired for selected representatives with serial 1:1 dilutions and duplicate data points, starting from 100 μM ligand concentration (with 0.4 μM protein, 20% LED power).

4.23. Ellman's assay

2 μM of the isolated β5i subunit of iCP (PSMB8 Human Protein, ProSpec-Tany TechnoGene Ltd., Ness-Ziona, Israel) in assay buffer (25 mM NaH₂PO₄, 0.1 mM EDTA, 150 mM NaCl, pH 6.6) was treated with 1000 μM of **84**, resulting in 1% DMSO concentration in the mixture. After 16 h incubation at 37 °C, 25 μL of thiol detection reagent in dry DMSO (Invitrogen, Ref No.: TC012-1 EA) was added to 100 μL of the sample. After brief shaking, the plate was incubated in dark at room temperature for 30 min, then fluorescence was measured in a microplate reader (BioTek Synergy Mx) (λ_{ex} = 390 nm and λ_{em} = 510 nm). Free thiol ratio (FTR%) and labelling ratio (LR%) values were calculated, as follows, then averaged for triplicated measurements:

$$\begin{aligned} \text{FTR}[\%] &= 100 \cdot \frac{\text{RFU}_{\text{sample}} - \text{RFU}_{\text{background}}}{\text{RFU}_{\text{DMSO}} - \text{RFU}_{\text{background}}} \quad \text{LR}[\%] \\ &= 100\% - \text{FTR}[\%] \end{aligned}$$

4.24. LC-MS measurements

The molecular weights of the conjugates of β5i were identified using a Triple TOF 5600+ hybrid Quadrupole-TOF LC/MS/MS system (AB Sciex LLC, Framingham, MA, USA) equipped with a Duo-Spray IonSource coupled with a Shimadzu Prominence LC20 UFLC (Shimadzu, Kyoto, Japan) system consisting of binary pump, an autosampler and a thermostated column compartment. Data acquisition and processing were performed using Analyst TF software version 1.7.1 (AB Sciex LLC, Framingham, MA, USA). Chromatographic separation was achieved on a Thermo Beta Basic C8 (50 mm × 2.1 mm, 3 μm, 150 Å) HPLC column. Sample was eluted in

gradient elution mode using solvent A (0.1% formic acid in water) and solvent B (0.1% formic acid in MeCN). The initial condition was 20% B for 1 min, followed by a linear gradient to 90% B by 4 min, from 5 to 6 min 90% B was retained; and from 6 to 6.5 min back to initial condition with 20% eluent B and retained from 6.5 to 9.0 min. Flow rate was set to 0.4 mL/min. The column temperature was 40 °C and the injection volume was 5 µL. Nitrogen was used as the nebulizer gas (GS1), heater gas (GS2), and curtain gas with the optimum values set at 30, 30 and 35 (arbitrary units), respectively. Data were acquired in positive electrospray mode in the mass range of $m/z = 300$ to 2500, with 1 s accumulation time. The source temperature was 350 °C and the spray voltage was set to 5500 V. Declustering potential value was set to 80 V. Peak View Software™ V.2.2 (AB Sciex LLC, Framingham, MA, USA) was used for deconvoluting the raw electrospray data to obtain the neutral molecular masses.

4.25. Molecular modelling

Compound preparations for docking included the generation of tautomeric and ionization states at pH 6–8 and the creation of 3D structures with LigPrep (Schrödinger Suite 2018-4, Schrödinger, LLC, New York, NY, 2018). The X-ray structure deposited as PDB entry 6E5B [55] was used for docking. The binding site is defined by the K and L chains, so all other chains were removed, as well as the covalently bound ligand. Protein Preparation Wizard [79,80] was used to add hydrogen atoms, protonate residues at pH 7, refine the H-bond network and to perform a restrained minimization. The receptor's grid box required for docking calculations was centered on the corresponding co-crystallized ligand. Covalent docking was performed with CovDock program using the pose prediction mode [80] with default setup.

4.26. Compound library

The compound library for initial screening contained 899 fragment-sized compounds. They were either purchased or synthesized in RCNS. Their molecular weight ranged from 103 to 372 with a median of 162, the calculated logP ranges from –3.0 to 3.3 with a median of 1.6, the number of hydrogen bond acceptors was between 0 and 3, the number of hydrogen bond donors was between 0 and 3, and the number of rotatable bonds was between 0 and 3. All properties were calculated by JChem for Excel (20.14.0.68; ChemAxon: Budapest, Hungary, 2020; Available online: <http://www.chemaxon.com>).

Author contributions

L.K. synthesized the compounds and wrote a manuscript draft; M.G. performed biochemical assays on proteasomes; B.S. synthesized the compounds; M.P. performed *in vitro* reactivity assays; P.A.-B. synthesized the compounds and helped with the design of compound library; L.P. performed labelling experiments; T.I. performed MS measurements; D.K. synthesized acrylamide derivatives; D.B. participated in the design of compounds and the library of compounds; G.G.F. performed computational methods, designed the compounds and the initial library, wrote a manuscript draft; S.G. coordinated the project, helped to write the manuscript and secured funding; G.M.K. coordinated the project, designed the *in house* compound library, secured funding and helped to write the manuscript; I.S. coordinated the project and wrote the manuscript.

Supporting information

Supporting Tables, Figures, Schemes, procedures for the

preparation of compounds **81** and **82**, molecular modeling of binding modes, as well as spectroscopic and analytical data for purchased compounds.

Declaration of competing interest

The authors declare that they have no known competing financial interests or personal relationships that could have appeared to influence the work reported in this paper.

Acknowledgments

This research was funded by the National Research Development and Innovation Office (grant number SNN_17 125496, 2018-2.1.11-TÉT-SI-2018-00005 and PD124598), by the Slovenian Research Agency (research core funding No. P1-0208, Grant N1-0068, and Grant J3-1745 to M.G.), and the Gedeon Richter Talentum Foundation. D. B. is supported by the János Bolyai Research Scholarship of the Hungarian Academy of Sciences. We thank Pál Szabó, Stane Pajk, and Maja Frelih for HRMS measurements, Dorottya Csányi for her contribution to NMR measurements, Adrienn Balla for her contribution to synthetic work and the Signal Transduction and Functional Genomics Research Group at RCNS, Budapest, for providing access to their MST device.

Abbreviations

UPS	ubiquitin-proteasome system; C
P	core particle
cCP	constitutive proteasome
iCP	immunoproteasome
RA	residual activity
SAR	structure-activity relationship;
TCDI	1,1'-thiocarbonyldiimidazole
ROS	reactive oxygen species
HRP-PR	horseradish peroxidase-phenol red
DTT	dithiothreitol
H2DCFDA	2',7'-dichlorodihydrofluorescein diacetate
TCEP	tris(2-carboxyethyl)phosphine;
GSH	glutathione
DTNB	5,5'-dithiobis-(2-nitrobenzoic acid)
TNB2-	5-mercapto-2-nitrobenzoic acid
HRMS	high-resolution mass spectrometry

Appendix A. Supplementary data

Supplementary data to this article can be found online at <https://doi.org/10.1016/j.ejmech.2021.113455>.

References

- [1] M.T. Michalek, E.P. Grant, C. Gramm, A.L. Goldberg, K.L. Rock, A role for the ubiquitin-dependent proteolytic pathway in MHC class I-restricted antigen presentation, *Nature* 363 (1993) 552–554, <https://doi.org/10.1038/363552a0>.
- [2] E.P. Grant, M.T. Michalek, A.L. Goldberg, K.L. Rock, Rate of antigen degradation by the ubiquitin-proteasome pathway influences MHC class I presentation, *J. Immunol.* 155 (8) (1995) 3750–3758.
- [3] B.M. Machiels, M.E. Henfling, W.L. Gerards, J.L. Broers, H. Bloemendal, F.C. Ramaekers, B. Schutte, Detailed analysis of cell cycle kinetics upon proteasome inhibition, *Cytometry* 28 (1997) 243–252, [https://doi.org/10.1002/\(SICI\)1097-0320\(19970701\)28:3<243::AID-CYTO9>3.0.CO;2-E](https://doi.org/10.1002/(SICI)1097-0320(19970701)28:3<243::AID-CYTO9>3.0.CO;2-E).
- [4] Y. Wu, H. Luo, N. Kanaan, J. Wu, The proteasome controls the expression of a proliferation-associated nuclear antigen ki-67, *J. Cell. Biochem.* 76 (4) (2000) 596–604.
- [5] Z. Chen, J. Hagler, V.J. Palombella, F. Melandri, D. Scherer, D. Ballard, T. Maniatis, Signal-induced site-specific phosphorylation targets IκBα to the ubiquitin-proteasome pathway, *Genes Dev.* 9 (13) (1995) 1586–1597, <https://doi.org/10.1101/gad.9.13.1586>.
- [6] D.C. Scherer, J.A. Brockman, Z. Chen, T. Maniatis, D.W. Ballard, Signal-induced

- degradation of I kappa B alpha requires site-specific ubiquitination, *Proc. Natl. Acad. Sci. U.S.A.* 92 (24) (1995) 11259–11263, <https://doi.org/10.1073/pnas.92.24.11259>.
- [7] J.F. Watkins, P. Sung, L. Prakash, S. Prakash, The *Saccharomyces cerevisiae* DNA repair gene RAD23 encodes a nuclear protein containing a ubiquitin-like domain required for biological function, *Mol. Cell Biol.* 13 (12) (1993) 7757–7765, <https://doi.org/10.1128/mcb.13.12.7757>.
- [8] C. Schaubert, L. Chen, P. Tongaonkar, I. Vega, D. Lambertson, W. Potts, K. Madura, Rad23 links DNA repair to the ubiquitin/proteasome pathway, *Nature* 391 (1998) 715–718, <https://doi.org/10.1038/246170a0>.
- [9] S.A. Shah, M.W. Potter, T.P. McDade, R. Ricciardi, R.A. Perugini, P.J. Elliott, J. Adams, M.P. Callery, 26S proteasome inhibition induces apoptosis and limits growth of human pancreatic cancer, *J. Cell. Biochem.* 82 (1) (2001) 110–122, <https://doi.org/10.1002/jcb.1150>.
- [10] R. Raynes, L.C.D. Pomatto, K.J.A. Davies, Degradation of oxidized proteins by the proteasome: distinguishing between the 20S, 26S, and immunoproteasome proteolytic pathways, *Mol. Aspect. Med.* 50 (2016) 41–55, <https://doi.org/10.1016/j.mam.2016.05.001>.
- [11] G.A. Collins, A.L. Goldberg, The logic of the 26S proteasome, *Cell* 169 (5) (2017) 792–806, <https://doi.org/10.1016/j.cell.2017.04.023>.
- [12] T.A. Thibadeau, D.M. Smith, A practical review of proteasome pharmacology, *Pharmacol. Rev.* 71 (2) (2019) 170–197, <https://doi.org/10.1124/pr.117.015370>.
- [13] M. Groll, L. Ditzel, J. Lowe, D. Stock, M. Bochtler, H.D. Bartunikt, R. Huber, Structure of 20S proteasome from yeast at 2.4 Å resolution, *Nature* 386 (1997) 463–471.
- [14] M. Groll, M. Bajorek, A. Köhler, L. Moroder, D.M. Rubin, R. Huber, M.H. Glickman, D. Finley, A gated channel into the proteasome core particle, *Nat. Struct. Biol.* 7 (11) (2000) 1062–1067, <https://doi.org/10.1038/80992>.
- [15] A. Köhler, P. Cascio, D.S. Leggett, K.M. Woo, A.L. Goldberg, D. Finley, The axial channel of the proteasome core particle is gated by the Rpt2 ATPase and controls both substrate entry and product release, *Mol. Cell* 7 (6) (2001) 1143–1152, [https://doi.org/10.1016/S1097-2765\(01\)00274-X](https://doi.org/10.1016/S1097-2765(01)00274-X).
- [16] L. Bedford, S. Paine, P.W. Sheppard, R.J. Mayer, J. Assembly Roelofs, Structure, and function of the 26S proteasome, *Trends Cell Biol.* 20 (7) (2010) 391–401, <https://doi.org/10.1016/j.tcb.2010.03.007>.
- [17] L. Budenholzer, C.L. Cheng, Y. Li, M. Hochstrasser, Proteasome structure and assembly, *J. Mol. Biol.* 429 (22) (2017) 3500–3524, <https://doi.org/10.1016/j.jmb.2017.05.027>.
- [18] C.S. Arendt, M. Hochstrasser, Identification of the yeast 20S proteasome catalytic centers and subunit interactions required for active-site formation, *Proc. Natl. Acad. Sci. U.S.A.* 94 (14) (1997) 7156–7161, <https://doi.org/10.1073/pnas.94.14.7156>.
- [19] D. Voges, P. Zwickl, W. Baumeister, The 26S proteasome: a molecular machine designed for controlled proteolysis, *Annu. Rev. Biochem.* 68 (1999) 1015–1068.
- [20] K. Tanaka, Role of proteasomes modified by interferon- γ in antigen processing, *J. Leukoc. Biol.* 56 (5) (1994) 571–575, <https://doi.org/10.1002/jlb.56.5.571>.
- [21] M. Aki, N. Shimbara, M. Takashina, K. Akiyama, S. Kagawa, T. Tamura, N. Tanahashi, T. Yoshimura, K. Tanaka, A. Ichihara, Interferon- γ induces different subunit organizations and functional diversity of proteasomes, *J. Biochem.* 115 (2) (1994) 257–269, <https://doi.org/10.1093/oxfordjournals.jbchem.a124327>.
- [22] D. Nandi, H. Jiang, J.J. Monaco, Identification of MECL-1 (LMP-10) as the third IFN- γ -inducible proteasome subunit, *J. Immunol.* 156 (7) (1996) 2361–2364.
- [23] M. Groettrup, C.J. Kirk, M. Basler, Proteasomes in immune cells: more than peptide producers? *Nat. Rev. Immunol.* 10 (1) (2010) 73–78, <https://doi.org/10.1038/nri2687>.
- [24] J.B. Almond, G.M. Cohen, The proteasome: a novel target for cancer chemotherapy, *Leukemia* 16 (2002) 433–443, <https://doi.org/10.1038/sj/leu/2402417>.
- [25] D.J. Kuhn, R.Z. Orlowski, The immunoproteasome as a target in hematologic malignancies, *Semin. Hematol.* 49 (3) (2012) 258–262, <https://doi.org/10.1053/j.seminhematol.2012.04.003>.
- [26] J.E. Park, Z. Miller, Y. Jun, W. Lee, K.B. Kim, Next-generation proteasome inhibitors for cancer therapy, *Transl. Res.* 198 (2018) 1–16, <https://doi.org/10.1016/j.trsl.2018.03.002>.
- [27] S. Ito, Proteasome inhibitors for the treatment of multiple myeloma, *Cancers* 12 (2) (2020) 265, <https://doi.org/10.3390/cancers12020265>.
- [28] E.E. Verbrugge, R.J. Schepers, W.F. Lems, T.D. de Gruijl, G. Jansen, Proteasome inhibitors as experimental therapeutics of autoimmune diseases, *Arthritis Res. Ther.* 17 (2015) 17, <https://doi.org/10.1186/s13075-015-0529-1>.
- [29] M. Basler, S. Mundt, A. Bitzer, C. Schmidt, M. Groettrup, The immunoproteasome: a novel drug target for autoimmune diseases, *Clin. Exp. Rheumatol.* 33 (1) (2015) 74–79.
- [30] C. Zhang, H. Zhu, J. Shao, R. He, J. Xi, R. Zhuang, J. Zhang, Immunoproteasome-selective inhibitors: the future of autoimmune diseases? *Future Med. Chem.* 12 (4) (2020) 269–272, <https://doi.org/10.4155/fmc-2019-0299>.
- [31] F. Limanaqi, F. Biagioni, A. Gaglione, C.L. Busceti, F. Fornai, A sentinel in the crosstalk between the nervous and immune system: the (Immuno)-Proteasome, *Front. Immunol.* 10 (2019) 628, <https://doi.org/10.3389/fimmu.2019.00628>.
- [32] E.M. Huber, M. Groll, Inhibitors for the immuno- and constitutive proteasome: current and future trends in drug development, *Angew. Chem. Int. Ed.* 51 (35) (2012) 8708–8720, <https://doi.org/10.1002/anie.201201616>.
- [33] A.F. Kisselev, M. Groettrup, Subunit specific inhibitors of proteasomes and their potential for immunomodulation, *Curr. Opin. Chem. Biol.* 23 (2014) 16–22, <https://doi.org/10.1016/j.cbpa.2014.08.012>.
- [34] P.M. Cromm, C.M. Crews, The proteasome in modern drug discovery: second life of a highly valuable drug target, *ACS Cent. Sci.* 3 (8) (2017) 830–838, <https://doi.org/10.1021/acscentsci.7b00252>.
- [35] N. Richey, D. Sarraf, X. Maréchal, N. Janmamode, R. Le Guével, E. Genin, M. Reboud-Ravaux, J. Vidal, Structure-based design of human immuno- and constitutive proteasomes inhibitors, *Eur. J. Med. Chem.* 145 (2018) 570–587, <https://doi.org/10.1016/j.ejmech.2018.01.013>.
- [36] D.J. Sherman, J. Li, Proteasome inhibitors: harnessing proteostasis to combat disease, *Molecules* 25 (3) (2020) 671, <https://doi.org/10.3390/molecules25030671>.
- [37] B.L. Zerfas, M.E. Maresch, D.J. Trader, The immunoproteasome: an emerging target in cancer and autoimmune and neurological disorders, *J. Med. Chem.* 63 (5) (2020) 1841–1858, <https://doi.org/10.1021/acs.jmedchem.9b01226>.
- [38] E.M. Huber, W. Heinemeyer, G. Bruin, H.S. Overkleeft, M. Groll, A umanized yeast proteasome identifies unique binding modes of inhibitors for the immunosubunit $\beta 5i$, *EMBO J.* 35 (23) (2016) 2602–2613, <https://doi.org/10.15252/emboj.201695222>.
- [39] E. Ogorevc, E.S. Schiffrer, I. Sosić, S. Gobec, A patent review of immunoproteasome inhibitors, *Expert Opin. Ther. Pat.* 28 (7) (2018) 517–540, <https://doi.org/10.1080/13543776.2018.1484904>.
- [40] R. Ettari, M. Zappalà, S. Grasso, C. Musolino, V. Innao, A. Allegra, Immunoproteasome-selective and non-selective inhibitors: a promising approach for the treatment of multiple myeloma, *Pharmacol. Ther.* 182 (2018) 176–192, <https://doi.org/10.1016/j.pharmthera.2017.09.001>.
- [41] J. Xi, R. Zhuang, L. Kong, R. He, H. Zhu, J. Zhang, Immunoproteasome-selective inhibitors: an overview of recent developments as potential drugs for hematologic malignancies and autoimmune diseases, *Eur. J. Med. Chem.* 182 (2019) 111646, <https://doi.org/10.1016/j.ejmech.2019.11.1646>.
- [42] I. Sosić, M. Gobec, B. Brus, D. Knez, M. Živec, J. Konc, S. Lešnik, M. Ogrizek, A. Obreza, D. Žigon, D. Janežič, I. Mlinarić-Rašćan, S. Gobec, Nonpeptidic selective inhibitors of the chymotrypsin-like ($\beta 5i$) subunit of the immunoproteasome, *Angew. Chem. Int. Ed.* 55 (19) (2016) 5745–5748, <https://doi.org/10.1002/anie.201600190>.
- [43] E.S. Schiffrer, I. Sosić, A. Šterman, J. Mravljak, I.M. Raščan, S. Gobec, M. Gobec, A focused structure-activity relationship study of psoralen-based immunoproteasome inhibitors, *Med. Chem. Commun.* 10 (11) (2019) 1958–1965, <https://doi.org/10.1039/c9md00365g>.
- [44] A. Scarpino, D. Bajusz, M. Proj, M. Gobec, I. Sosić, S. Gobec, G.G. Ferenczy, G.M. Keresű, Discovery of immunoproteasome inhibitors using large-scale covalent virtual screening, *Molecules* 24 (2019) 2590.
- [45] H. Fan, N.G. Angelo, J.D. Warren, C.F. Nathan, G. Lin, Oxathiazolones selectively inhibit the human immunoproteasome over the constitutive proteasome, *ACS Med. Chem. Lett.* 5 (4) (2014) 405–410, <https://doi.org/10.1021/ml400531d>.
- [46] V. Kasam, N.R. Lee, K.B. Kim, C.G. Zhan, Selective immunoproteasome inhibitors with non-peptide scaffolds identified from structure-based virtual screening, *Bioorg. Med. Chem. Lett.* 24 (15) (2014) 3614–3617, <https://doi.org/10.1016/j.bmcl.2014.05.025>.
- [47] H. Cui, R. Baur, C. Le Chapelain, C. Dubiella, W. Heinemeyer, E.M. Huber, M. Groll, Structural elucidation of a nonpeptidic inhibitor specific for the human immunoproteasome, *Chembiochem* 18 (6) (2017) 523–526, <https://doi.org/10.1002/cbic.201700021>.
- [48] E. Bosc, J. Nastri, V. Lefort, M. Valli, F. Contiguiba, R. Pioli, M. Furlan, V. da S. Bolzani, C. El Amri, M. Reboud-Ravaux, Piperlongumine and some of its analogs inhibit selectively the human immunoproteasome over the constitutive proteasome, *Biochem. Biophys. Res. Commun.* 496 (3) (2018) 961–966, <https://doi.org/10.1016/j.bbrc.2018.01.100>.
- [49] G. de Bruin, E.M. Huber, B.T. Xin, E.J. Van Rooden, K. Al-Ayed, K.B. Kim, A.F. Kisselev, C. Driessen, M. Van Der Stelt, G.A. Van Der Marel, M. Groll, H.S. Overkleeft, Structure-based design of $\beta 1i$ or $\beta 5i$ specific inhibitors of human immunoproteasomes, *J. Med. Chem.* 57 (14) (2014) 6197–6209, <https://doi.org/10.1021/jm500716s>.
- [50] H.W.B. Johnson, J.L. Anderl, E.K. Bradley, J. Bui, J. Jones, S. Arastu-Kapur, L.M. Kelly, E. Lowe, D.C. Moebius, T. Muchamuel, C. Kirk, Z. Wang, D. McMinn, Discovery of highly selective inhibitors of the immunoproteasome low molecular mass polypeptide 2 (LMP2) subunit, *ACS Med. Chem. Lett.* 8 (4) (2017) 413–417, <https://doi.org/10.1021/acsmchemlett.6b00496>.
- [51] D. Bhattarai, M.J. Lee, A. Baek, I.J. Yeo, Z. Miller, Y.M. Baek, S. Lee, D.E. Kim, J.T. Hong, K.B. Kim, LMP2 inhibitors as a potential treatment for Alzheimer's disease, *J. Med. Chem.* 63 (7) (2020) 3763–3783, <https://doi.org/10.1021/acsmchemlett.0c00416>.
- [52] R. Ettari, C. Cerchia, S. Maiorana, M. Guccione, E. Novellino, A. Bitto, S. Grasso, A. Lavecchia, M. Zappalà, Development of novel amides as noncovalent inhibitors of immunoproteasomes, *ChemMedChem* 14 (8) (2019) 842–852, <https://doi.org/10.1002/cmdc.201900028>.
- [53] G. de Bruin, B.T. Xin, M. Kraus, M. Van Der Stelt, G.A. Van Der Marel, A.F. Kisselev, C. Driessen, B.I. Florea, H.S. Overkleeft, A set of activity-based

- probes to visualize human (Immuno)Proteasome activities, *Angew. Chem. Int. Ed.* 55 (13) (2016) 4199–4203, <https://doi.org/10.1002/anie.201509092>.
- [54] H.W.B. Johnson, E. Lowe, J.L. Anderl, A. Fan, T. Muchamuel, S. Bowers, D.C. Moebius, C. Kirk, D.L. McMinn, Required immunoproteasome subunit inhibition profile for anti-inflammatory efficacy and clinical candidate KZR-616 ((2S,3R)-N-((S)-3-(Cyclopent-1-En-1-yl)-1-((R)-2-Methyloxiran-2-yl)-1-Oxopropan-2-yl)-3-Hydroxy-3-(4-Methoxyphenyl)-2-((S)-2-(2-Morpholin, *J. Med. Chem.* 61 (24) (2018) 11127–11143, <https://doi.org/10.1021/acs.jmedchem.8b01201>.
- [55] E. Ladi, C. Everett, C.E. Stivala, B.E. Daniels, M.R. Durk, S.F. Harris, M.P. Huestis, H.E. Purkey, S.T. Staben, M. Augustin, M. Blaesse, S. Steinbacher, C. Eidenschen, R. Pappu, M. Siu, Design and evaluation of highly selective human immunoproteasome inhibitors reveal a compensatory process that preserves immune cell viability, *J. Med. Chem.* 62 (15) (2019) 7032–7041, <https://doi.org/10.1021/acs.jmedchem.9b00509>.
- [56] E.S. Karreci, H. Fan, M. Uehara, A.B. Mihali, P.K. Singh, A.T. Kurdi, Z. Solhjou, L.V. Riella, I. Ghobrial, T. Laragione, S. Routray, J.P. Assaker, R. Wang, G. Sukenick, L. Shi, F.J. Barrat, C.F. Nathan, G. Lin, J. Azzi, Brief treatment with a highly selective immunoproteasome inhibitor promotes long-term cardiac allograft acceptance in mice, *Proc. Natl. Acad. Sci. U.S.A.* 113 (52) (2016) E8425–E8432, <https://doi.org/10.1073/pnas.1618548114>.
- [57] D.A. Erlanson, I.J.P. De Esch, W. Jahnke, C.N. Johnson, P.N. Mortenson, Fragment-to-Lead medicinal chemistry publications in 2018, *J. Med. Chem.* 63 (9) (2020) 4430–4444, <https://doi.org/10.1021/acs.jmedchem.9b01581>.
- [58] H. Khan, A. Badshah, F. Shaheen, C. Gieck, R.A. Qureshi, 1-Methyl-1H-Benzimidazole-2(3H)-Thione, *Acta Crystallogr. E* 64 (2008) o1141, <https://doi.org/10.1107/S1600536808015043>.
- [59] M. Proj, I. Sosić, S. Gobec, Synthesis and NMR spectroscopic assignment of chlorinated benzimidazole-2-thione derivatives, *Tetrahedron Lett.* 60 (39) (2019) 151078, <https://doi.org/10.1016/j.tetlet.2019.151078>.
- [60] R.S. Balestrero, D.M. Forkey, J.G. Russell, 15N NMR: iminothiol-thioamide Tautomerism of 2-mercaptobenzazoles and 1-methyl-2-mercaptoimidazole, *Magn. Reson. Chem.* 24 (8) (1986) 651–655, <https://doi.org/10.1002/mrcc.1260240803>.
- [61] C. Abbehausen, R.E.F. De Paiva, A.L.B. Formiga, P.P. Corbi, Studies of the tautomeric equilibrium of 1,3-thiazolidine-2-thione: theoretical and experimental approaches, *Chem. Phys.* 408 (2012) 62–68, <https://doi.org/10.1016/j.chemphys.2012.09.019>.
- [62] J. Boström, D.G. Brown, R.J. Young, G.M. Keserü, Expanding the medicinal chemistry synthetic toolbox, *Nat. Rev. Drug Discov.* 17 (10) (2018) 709–727, <https://doi.org/10.1038/nrd.2018.116>.
- [63] C. Aldrich, C. Bertozzi, G.I. Georg, L. Kiessling, C. Lindsley, D. Liotta, K.M. Merz, A. Schepartz, S. Wang, The ecstasy and agony of assay interference compounds, *ACS Cent. Sci.* 3 (2017) 143–147, <https://doi.org/10.1021/acscentsci.7b00069>.
- [64] P.A. Johnston, K.M. Soares, S.N. Shinde, C.A. Foster, T.Y. Shun, H.K. Takyi, P. Wipf, J.S. Lazo, Development of a 384-well colorimetric assay to quantify hydrogen peroxide generated by the redox cycling of compounds in the presence of reducing agents, *Assay Drug Dev. Technol.* 6 (4) (2008) 505–518, <https://doi.org/10.1089/adt.2008.151>.
- [65] B. Mirković, I. Sosić, S. Gobec, J. Kos, Redox-based inactivation of cysteine cathepsins by compounds containing the 4-aminophenol moiety, *PLoS One* 6 (11) (2011), e27197, <https://doi.org/10.1371/journal.pone.0027197>.
- [66] L.A. Lor, J. Schneck, D.E. McNulty, E. Diaz, M. Brandt, S.H. Thrall, B. Schwartz, A simple assay for detection of small-molecule redox activity, *J. Biomol. Screen* 12 (6) (2007) 881–890, <https://doi.org/10.1177/1087057107304113>.
- [67] E. Resnick, A. Bradley, J. Gan, A. Douangamath, T. Krojer, R. Sethi, P.P. Geurink, A. Aimon, G. Amitai, D. Bellini, J. Bennett, M. Fairhead, O. Fedorov, R. Gabizon, J. Gan, J. Guo, A. Plotnikov, N. Reznik, G.F. Ruda, L. Díaz-Sáez, V.M. Straub, T. Szommer, S. Velupillai, D. Zaidman, Y. Zhang, A.R. Coker, C.G. Dowson, H.M. Barr, C. Wang, K.V.M. Huber, P.E. Brennan, H. Ovaas, F. Von Delft, N. London, Rapid covalent-probe discovery by electrophile-fragment screening, *J. Am. Chem. Soc.* 141 (22) (2019) 8951–8968, <https://doi.org/10.1021/jacs.9b02822>.
- [68] C. Dubiella, R. Baur, H. Cui, E.M. Huber, M. Groll, Selective inhibition of the immunoproteasome by structure-based targeting of a non-catalytic cysteine, *Angew. Chem. Int. Ed.* 54 (52) (2015) 15888–15891, <https://doi.org/10.1002/anie.201506631>.
- [69] S.G. Kathman, A.V. Statsyuk, Covalent tethering of fragments for covalent probe discovery, *Med. Chem. Commun.* 7 (4) (2016) 576–585, <https://doi.org/10.1039/c5md00518c>.
- [70] E.P. Harvey, Z.J. Hauseman, D.T. Cohen, T.J. Rettenmaier, S. Lee, A.J. Huhn, T.E. Wales, H.S. Seo, J. Luccarelli, C.E. Newman, R.M. Guerra, G.H. Bird, S. Dhe-Paganon, J.R. Engen, J.A. Wells, L.D. Walensky, Identification of a covalent molecular inhibitor of anti-apoptotic BFL-1 by disulfide tethering, *Cell Chem. Biol.* 27 (6) (2020) 647–656, <https://doi.org/10.1016/j.chembiol.2020.04.004>.
- [71] H.F. Motiwala, Y.H. Kuo, B.L. Stinger, B.A. Palfey, B.R. Martin, Tunable heteroaromatic sulfones enhance in-cell cysteine profiling, *J. Am. Chem. Soc.* 142 (4) (2020) 1801–1810, <https://doi.org/10.1021/jacs.9b08831>.
- [72] T. Kantner, A.G. Watts, Characterization of reactions between water-soluble trialkylphosphines and thiol alkylating reagents: implications for protein-conjugation reactions, *Bioconjugate Chem.* 27 (10) (2016) 2400–2406, <https://doi.org/10.1021/acs.bioconjchem.6b00375>.
- [73] S. Fitzjohn, M.P. Robinson, M.D. Turnbull, A.M. Smith, R. Salmon, R. Taylor, *Heterocyclic Compounds, US Patent 5451594A*, 1995.
- [74] M. Mochizuki, M. Kori, K. Kobayashi, T. Yano, Y. Sako, M. Tanaka, N. Kanzaki, A.C. Gyorkos, C.P. Corrette, S.Y. Cho, S.A. Pratt, K. Aso, Design and synthesis of benzimidazoles as novel corticotropin-releasing factor 1 receptor antagonists, *J. Med. Chem.* 59 (6) (2016) 2551–2566, <https://doi.org/10.1021/acs.jmedchem.5b01715>.
- [75] M. Hahn, E.-M. Becker, A. Knorr, D. Schneider, J.-P. Stasch, K.-H. Schlemmer, F. Wunder, F. Stoll, S. Heitmeier, K. Münster, N. Griebenow, T. Lampe, S. El Sheikh, V. Min-jian Li, *Oxo-Heterocyclic Substituted Carboxylic Acid Derivatives and the Use Thereof, US Patent 2011/0034450A1*, 2011.
- [76] L. Wimmer, M. Parmentier, B. Riss, T. Kapferer, C. Ye, L. Li, H. Kim, J. Li, Water-promoted chlorination of 2-mercaptobenzothiazoles, *Synth. Met.* 50 (10) (2018) 2027–2032, <https://doi.org/10.1055/s-0036-1591553>.
- [77] M. Hasegawa, N. Nishigaki, Y. Washio, K. Kano, P.A. Harris, H. Sato, I. Mori, R.I. West, M. Shibahara, H. Toyoda, L. Wang, R.T. Nolte, J.M. Veal, M. Cheung, Discovery of novel benzimidazoles as potent inhibitors of TIE-2 and VEGFR-2 tyrosine kinase receptors, *J. Med. Chem.* 50 (18) (2007) 4453–4470, <https://doi.org/10.1021/jm0611051>.
- [78] I. Egle, I. Methvin, R. Urbanek, F.M. McLaren, S.B. Walsh, G.B. Steelman, D.G. Brown, D. Nugiel, D.W. Chen, A. Slassi, M. Fupeng, *Bicyclic Benzimidazole Compounds and Their Use as Metabotropic Glutamate Receptor Potentiators, US Patent 2009/192169A1*, 2009.
- [79] G. Madhavi Sastry, M. Adzhigirey, T. Day, R. Annabhimoju, W. Sherman, Protein and ligand preparation: parameters, protocols, and influence on virtual screening enrichments, *J. Comput. Aided Mol. Des.* 27 (3) (2013) 221–234, <https://doi.org/10.1007/s10822-013-9644-8>.
- [80] K. Zhu, K.W. Borrelli, J.R. Greenwood, T. Day, R. Abel, R.S. Farid, E. Harder, Docking covalent inhibitors: a parameter free approach to pose prediction and scoring, *J. Chem. Inf. Model.* 54 (7) (2014) 1932–1940, <https://doi.org/10.1021/ci500118s>.
- [81] Aaron Keeley, *Arch. Pharm.* (2018), <https://doi.org/10.1002/ardp.201800184>.